AN EXPERIMENTAL AND MODELING STUDY OF THE PHOTOCHEMICAL OZONE REACTIVITY OF ACETONE

Final Report to

Chemical Manufacturers Association
Contract No. KET-ACE-CRC-2.0

by

William P. L. Carter,
Dongmin Luo, Irina L. Malkina and John A. Pirece

December 10, 1993

Statewide Air Pollution Research Center, and
College of Engineering Center for Environmental Research and Technology
University of California
Riverside, California 92521

SUMMARY

A series of environmental chamber experiments and computer model simulations were carried out to assess the tendency of acetone to promote ozone formation in photochemical smog. The experiments consisted of NO_x - air photolysis of acetone by itself, and determinations of the effect of adding acetone on ozone formation in model photochemical smog systems. Indoor chambers using either fluorescent blacklight or xenon arc light sources and an outdoor chamber utilizing sunlight were employed. Similar experiments utilizing acetaldehyde were carried out for comparison and control purposes. The gas-phase photochemical mechanism for the atmospheric reactions of acetone was updated and was evaluated by model simulations of the results of these experiments. The mechanism was found to overpredict the effect of acetone on ozone formation and radical levels in the indoor chamber experiments with the blacklight light source and in some of the outdoor chamber runs, but fit the results of other outdoor chamber runs and the experiments runs using the xenon arc light source reasonably well. An adjusted mechanism which gave better agreement with the blacklight experiments and with some of the outdoor runs was developed.

The updated and adjusted acetone mechanisms were then used in model calculations to assess the effects of acetone on ozone formation under atmospheric conditions. This was done by calculating its incremental reactivity (defined as amount of additional ozone formed caused by adding acetone to the emissions, divided by the amount added) in model scenarios representing ozone episodes in 39 urban areas around the United States. The incremental reactivities of ethane and a mixture representing total emissions reactive organic gases from all sources were also calculated for comparison. The results indicate that acetone forms 10-15% as much ozone on a per mass basis as total ROG emissions, while ethane forms 6-20% as much ozone, depending on conditions. The implications of these results on the question of whether acetone should be exempt from regulation as an ozone precursor are discussed.

ACKNOWLEDGEMENTS AND DISCLAIMERS

The authors wish to acknowledge and thank our project officer, Dr. David Morgott of Eastman Kodak Co. for many helpful discussions and his support of this work. We also acknowledge Mr. William Long for valuable assistance in carrying out the experiments, Mr. Ken Sasaki for assistance in developing the outdoor chamber light model, Mr. Dennis Fitz for assisting in the management of this program and reviewing parts of this report, Ms. Kathalena Smihula, Mr. Armando Avallone, Mr. Patrick Sekera, and Mr. Jeff Friend for assisting in carrying out the experiments, and to Dr. Joseph Norbeck, the director of the College of Engineering, Center for Environmental Research and Technology, for supporting the student assistants working on this program and for providing some of the equipment which was used.

The experiments with acetone were funded by the CMA in part through providing support to Coordinating Research Council Project No. ME-9, and in part through Contract No. KET-ACE-CRC-2.0. Some of the base case and control experiments used in the data analysis and modeling for this program were obtained under funding from the California Air Resources Board Contract No. A032-0692 and Coordinated Research Council Project No. ME-9. In addition, the xenon arc light source used in this study was funded by the National Renewable Energy Laboratory through Contract No. XZ-2-12075-1, and the modular building where most of the experiments were conducted were provided by the California South Coast Air Quality Management District through Contract No. C91323. We wish to thank these agencies for their support of our programs.

The opinions and conclusions in this report are entirely those of the primary author, Dr. William P. L. Carter. Mention of trade names or commercial products do not constitute endorsement or recommendation for use.

EXECUTIVE SUMMARY

Background

Photochemical ozone formation is caused by the gas phase reactions of volatile organic compounds (VOCs) with oxides of nitrogen (NO_x) in the presence of sunlight. To reduce ground level ozone and achieve air quality standards, emissions of both NO_x and VOCs are subject to controls. However, VOCs are not equal in the amount of ozone formation they cause. If a VOC can be shown to make a negligible contribution to ozone formation when it is emitted into the atmosphere, the United States Environmental Protection Agency (EPA) can exempt it from regulation as an ozone precursor. Although the EPA has no formal policy as to what constitutes "negligible" reactivity, it has the informal policy of using the reactivity of ethane as the standard because ethane is the most rapidly reacting of the compounds which has already been exempted. Thus if a compound forms comparable or less ozone on a per gram emitted basis than ethane it can be considered for exemption.

Acetone is an important solvent species which reacts sufficiently slowly that it might reasonably be considered as a candidate for exemption. Its net atmospheric reaction rate, on a mass basis, has been estimated to be slightly less than that of ethane. However, the rate at which a VOC reacts is not the only factor which determine its effect on ozone. Unlike ethane, acetone undergoes photodecomposition in the atmosphere to form radicals, and increasing radical levels tends to cause increased rates of ozone formation from the other VOCs present. If this effect were sufficiently important, it would mean that acetone would cause more ozone formation than ethane.

The most direct quantitative measure of the degree to which a VOC contributes to ozone formation in a photochemical air pollution episode is its "incremental reactivity" for that episode. This is defined as the amount of additional ozone formation resulting from the addition of a small amount of the VOC to the emissions in the episode, divided by the amount of compound added. This measure of reactivity takes into account all of the factors by which a VOC affects ozone formation, including the effect of the environment where the VOC reacts. The latter is important because the amount of ozone formation caused by the reactions of a VOC depends significantly on how much NO_x is present.

We have previously investigated methods for ranking photochemical reactivities of various VOCs by calculating incremental reactivities of different VOCs under varying NO_x conditions in model scenarios representing various urban areas in the United States. Depending on the NO_x conditions used, acetone was calculated to be of comparable or greater reactivity than ethane. However, the chemical mechanism used for acetone in these calculations has not been adequately experimentally verified, and thus it would

not be appropriate to use these previous results as a basis for deciding whether it is appropriate to exempt acetone from regulation as an ozone precursor.

This report describes a study designed to provide experimental data necessary to test and improve the reliability of the atmospheric chemical mechanism for acetone, and then use the experimentally-verified mechanism to re-evaluate the atmospheric reactivity of acetone relative to those of ethane and other VOCs.

Experimental Approach

A number of different types of environmental chamber experiments were carried out to evaluate various aspects of acetone's atmospheric reaction mechanism. These are summarized below:

Acetone - NO_x experiments consisted of irradiations where acetone was the only compound present in sufficient quantities to form ozone. This provides the simplest and most direct test of acetone's mechanisms. For control purposes, similar experiments were carried out using acetaldehyde instead of acetone.

Incremental Reactivity experiments consisted of irradiations, in the presence of NO_x, of a reactive organic gas (ROG) "surrogate" mixture designed to represent ROG pollutants in ambient air, alternating (or simultaneously) with irradiations of the same mixture with varying amounts of acetone added. This provides the most direct test of a mechanism's ability to simulate acetone's incremental reactivity. For control purposes, similar experiments were carried out using acetaldehyde. In addition, relevant results of incremental reactivity experiments with ethane, carried out in a previous study, are also summarized in this report.

Experiments with varying light sources were carried out to test the mechanism for acetone under varying lighting conditions. This is important because one of the main factors affecting acetone's reactivity is the fact that it undergoes photolysis. The light sources used were blacklights, xenon arc lights, and (in outdoor chamber experiments) natural sunlight.

Direct acetone vs ethane comparison experiments consisted of irradiations of a ROG surrogate - NO_x mixture with added acetone simultaneously with irradiations of the same mixture with a comparable amount of added ethane on the other side. Although such experiments do not necessarily indicate the relative reactivity of acetone and ethane in the atmosphere (because incremental reactivities depend on conditions, and conditions in the chamber are different than in the atmosphere), they were conducted to provide a comparison with similar experiments carried out at the University of North Carolina.

Chemical Mechanism Development

As part of this work, we also re-examined the literature concerning the atmospheric reactions of acetone. The mechanism for its reaction with OH radicals was modified to be consistent with recent laboratory results. The experimental data from which acetone's photolysis quantum yields were derived were evaluated and modeled, and some corrections were made based on the results of this analysis. The resulting updated mechanism predicted a slightly lower reactivity for acetone in the atmosphere than the one used previously. This updated mechanism was then evaluated by conducting model simulations of the experiments discussed above.

Experimental and Mechanism Evaluation Results

The updated mechanism was found to simulate reasonably well the results of the experiments using the indoor chamber light source most closely resembling sunlight and the outdoor chamber runs that were conducted during the summer. However, this mechanism consistently overpredicted the rate of ozone formation in the blacklight chamber experiments and also overpredicted the ozone formation in the wintertime acetone - NO_x run in the outdoor chamber. It is unlikely that this is due to incorrect characterization of the blacklight intensity or spectra, because the model provides good simulations of the photochemical reactivity of acetaldehyde, a VOC that photolyzes in a similar wavelength region as acetone. Thus, it appears likely that the problem is that the model incorrectly represents how the acetone photolysis quantum yields depend on wavelength.

An adjusted version of the updated acetone mechanism was developed that was considerably more successful in simulating the experiments conducted in this study. The adjustment involves assuming that the quantum yields fall off with increasing wavelength much more rapidly than indicated in previous work, but that the fall off begins at a slightly longer wavelength. Although this adjustment is not theoretically unreasonable, there is no basis for it other than fitting these environmental chamber data, which are highly complex chemical systems with a number of other potential sources of error. The possibility that the problem may be due to an incorrect characterization of the effect of the mercury lines in the blacklight light source cannot be entirely ruled out. Therefore, in the assessment of the reactivities of acetone in the atmosphere, we have used both the unadjusted (or standard) and the adjusted acetone mechanism in the model calculations.

Atmospheric Reactivity Calculations

The adjusted and unadjusted updated acetone mechanisms were then used in model calculation to assess the effects of acetone on ozone formation under atmospheric conditions. The incremental reactivity of acetone, ethane, and the base ROG mixture (the mixture representing the sum of all VOCs emitted into the atmosphere) were calculated in model scenarios representing ozone episodes in 39 urban areas throughout the United States. It was found that the adjustment to the acetone quantum yields to fit our chamber data caused an approximately 13% reduction in its incremental reactivity calculated for these

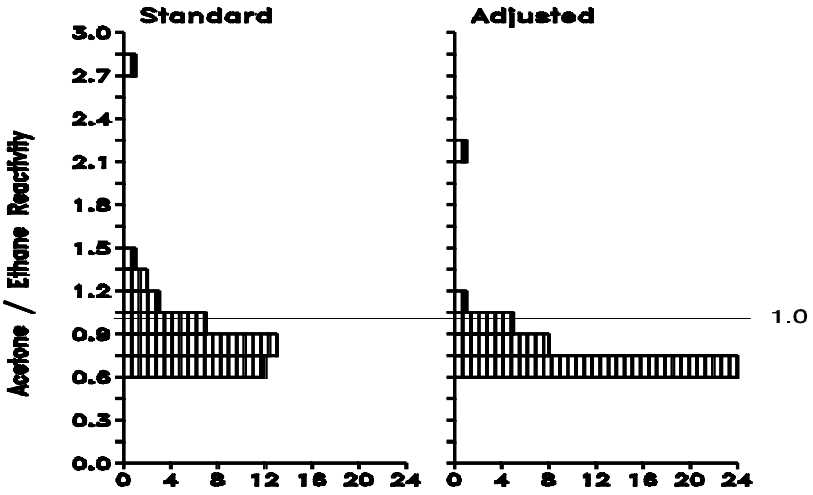

Figure EX-1. Distribution plots of incremental reactivities of acetone (standard and adjusted mechanisms) relative to ethane. Based on O_3 yields per gram VOC.

model scenarios. This is a relatively small effect compared to the extent to which the relative reactivity of acetone varied with atmospheric conditions. Thus, it is concluded that, although there are uncertainties in acetone's quantum yields, the effect of this uncertainty is not so large that it should substantively affect conclusions concerning the range of acetone's effect on ozone production under conditions represented by the model scenarios we employed.

Figure EX-1 shows distribution plots of the reactivity of acetone relative to that of ethane in the 39 scenarios, where reactivity is quantified by yield of ozone formed per gram of VOC emitted. The acetone/ethane reactivity ratio can be seen to vary among the scenarios, though in a majority of cases acetone is slightly less reactive than ethane. However, in one scenario, which represents unusually high NO_x conditions, acetone was calculated to be 2-3 times more reactive than ethane, depending on which acetone mechanism was used. As discussed below, this is due entirely to the unusually low reactivity of ethane in that scenario.

A more relevant measure of reactivity in control strategy applications is the incremental reactivity of the VOC relative to that of the sum of all ROG emissions, or the "relative reactivity". Distribution plots of the relative reactivities of acetone and ethane are shown in Figure EX-2. When looked at this way, it can be seen that the relative reactivity of ethane is far more variable than that of acetone. Thus the variability of the acetone/ethane ratio can be attributed almost entirely to the variability of the reactivity of ethane. For example, the scenario with the unusually high acetone/ethane ratio has the lowest relative reactivity for ethane but a near-average value for acetone. While the relative reactivity for ethane is as high as 0.24 under some circumstances, it is never higher than 0.18 for acetone, even

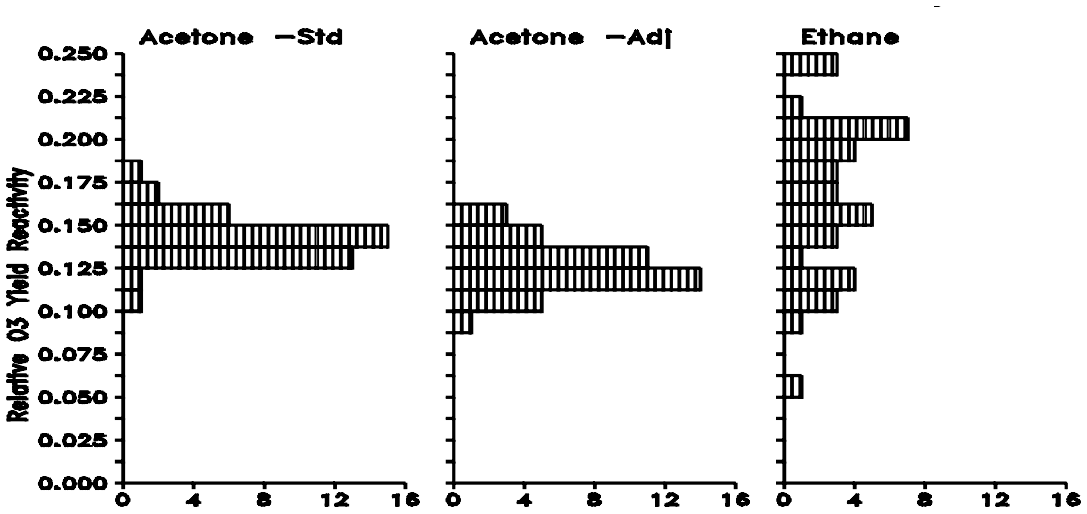

Figure EX-2. Distribution plots of relative reactivities of acetone and ethane. Based on O_3 yields per gram VOC.

using the more reactive standard mechanism for acetone. Conversely, while the relative reactivity for ethane is as low as 0.05, it is never lower than 0.11 for acetone using the standard mechanism. Thus, the relative reactivity range of acetone falls entirely within the range for ethane.

Conclusions

Although there are uncertainties in acetone's atmospheric photooxidation mechanism, the experiments and model simulations carried out in this work indicate that these uncertainties are not large enough to substantially affect conclusions concerning acetone's ozone formation potential relative to ethane or other VOCs. The standard and the adjusted acetone mechanisms can be thought of as giving respectively the upper and the lower estimates of acetone's likely reactivity in any particular scenario. The differences between these two estimates were small compared to the variability of acetone's relative reactivity from scenario to scenario.

The difference in acetone's reactivity relative to ethane was also found to be less than the variability of their relative reactivities from scenario to scenario. This variability is due more to the variability of the reactivity of ethane with scenario conditions than that for acetone. On this basis, it can be concluded the acetone and ethane can be considered to have essentially the same reactivity to within their variability with environmental conditions.

We recommend, however, that a comparison of the reactivities of acetone and ethane not be used as the sole basis for determining whether acetone should be exempt from regulation as an ozone precursor. In considering whether a compound should be exempt, it is appropriate to assess its reactivity relative to

the mixture of all VOC emissions. When EPA decided to exempt ethane, it effectively decided that it was not necessary to regulate emissions of a VOC that could be almost 25% as reactive as the average of all VOC emissions in terms of peak ozone concentrations, and almost 20% as reactive in terms of effect on integrated ozone over the ambient ozone standard. When looked at this way, exempting a compound that is calculated to be no more than 20% as reactive in terms of peak ozone, or 15% as reactive in terms of integrated ozone over the standard, does not appear to be an inconsistent policy.

TABLE OF CONTENTS

LIST OF TABLES

LIST OF FIGURES

INTRODUCTION

Background

Photochemical ozone formation is caused by the gas phase reactions of volatile organic compounds (VOCs) with oxides of nitrogen (NO_x) emitted into the atmosphere. To reduce ground level ozone and achieve air quality standards, emissions of both NO_x and VOCs are subject to controls. However, VOCs are not equal in the amount of ozone formation they cause. If a VOC can be shown to make a negligible contribution to ozone formation when it is emitted into the atmosphere, the United States Environmental Protection Agency (EPA) can exempt it from regulation as an ozone precursor. Although the EPA has no formal policy as to what constitutes "negligible" reactivity, it has the informal policy of using the reactivity of ethane as the standard because ethane is the most rapidly reacting of the compounds which has already been exempted. Thus if a compound forms comparable or less ozone on a per gram emitted basis than ethane it can be considered for exemption. The bases for the decisions to exempt ethane but not compounds more reactive than it has not been made clear, and they are probably largely subjective. However, the existing precedent provides a guideline for evaluating possible exemption of additional compounds which is relatively straightforward as long as the candidate compound is not of comparable reactivity as ethane.

Acetone is an important solvent species which reacts fairly slowly in the atmosphere, and thus might reasonably be considered as a candidate for exemption. Exempting acetone from regulation as an ozone precursor would encourage its substitution for more reactive solvent species such as toluene, and permit its use as a replacement for ozone depleters and greenhouse gases such as CFC-11, methyl chloroform and methylene chloride (Eastman Chemical and Hoechst Celanese, 1993). Acetone is also an example of a VOC which might be considered to have comparable reactivity as ethane. Meyrahn et al. (1986) estimated the average annual atmospheric half life of acetone to be 22 days, which can be compared to 25 days calculated for ethane for the same conditions. Acetone reacts with OH radicals ~15% slower than ethane (Atkinson, 1989), but unlike ethane it is also consumed by photolysis, resulting in an overall half life which is essentially the same as that for ethane to within the uncertainties of the estimates. However, acetone has a higher molecular weight than ethane, which means that fewer molecules of acetone react per unit mass emitted. This makes acetone slightly less reactive than ethane by this standard. Thus acetone would be a viable candidate for exemption by the ethane standard if the only criterion used is the rate the compounds react in the atmosphere.

However, the rate at which a VOC reacts in the atmosphere is only one of several factors which determines its effect on ozone formation (Carter and Atkinson, 1989; Carter, 1991, 1993a,b; Carter et al., 1993a,b; Jeffries and Crouse, 1991). Other factors include the amount of ozone formed once a VOC

reacts, the effect of the VOC's reactions on the reactions of other VOCs, and the effects of the reactions of the VOC's reaction products. (Carter and Atkinson, 1989; Carter et al., 1993a,b). For example, if a VOC's reactions (or those of its products) tend to promote radical levels in the atmosphere, then they would increase the rates of reactions of all the VOCs present, and the rate of ozone formation from these reactions. Because acetone photolysis is expected to form radicals (Atkinson, 1990; Meyrahn et al., 1986, and references therein), acetone may have a greater effect on ozone than expected based on its reaction rate alone.

The most direct quantitative measure of the degree to which a VOC contributes to ozone formation in a photochemical air pollution episode is its "incremental reactivity" for that episode. This is defined as the amount of additional ozone formation resulting from the addition of a small amount of the VOC to the emissions in the episode, divided by the amount of compound added. This measure of reactivity takes into account all of the factors by which a VOC affects ozone formation, including the effect of the environment where the VOC reacts. The latter is important because the amount of ozone formation caused by the reactions of a VOC depends significantly on how much NO_x is present. If NO_x is absent, no ozone is formed and all VOCs have incremental reactivities of zero. Under low NO_x conditions, ozone is NO_x-limited, and aspects of a VOCs mechanism affecting NO_x removal rates are important in affecting incremental reactivity. Under sufficiently high NO_x conditions, ozone yields are determined by how rapidly ozone is formed, and therefore aspects of the mechanism affecting overall radical levels tend to be highly important.

Methods for ranking photochemical reactivities of various VOCs have been investigated by calculating incremental reactivities of different VOCs under varying NO_x conditions in model scenarios representing 39 different urban ozone non-attainment areas in the United States (Carter, 1991; 1993a,b). Several different incremental reactivity scales were developed, based on different NO_x conditions and different methods for measuring O_3 impacts. These include the Maximum Incremental Reactivity (MIR) scale, which reflects effects of VOCs on ozone yields under relatively high NO_x conditions where VOCs have their greatest effect on ozone, and the Maximum Ozone Incremental Reactivity (MOIR) scale, which reflects effects of VOCs on ozone yields under the somewhat lower NO_x conditions which are optimum for formation of peak ozone concentrations. In addition, various "base case" reactivity scales were developed to reflect (using various averaging or weighting methods) the distribution of incremental reactivities under the varying NO_x conditions associated with the different urban areas. These tended to give similar rankings as the MIR or MOIR scales, depending on the derivation or ozone quantification method used (Carter, 1991; 1993a,b).

The incremental reactivity of acetone (in terms of ozone per gram) was previously calculated to be slightly less than that of ethane in the MOIR scale, but was 2-3 times greater than that of ethane in the MIR scale. Thus the calculations indicate that the reactivity of acetone relative to ethane depends on NO_x

conditions (Carter, 1993a,b). However, this factor of 2-3 maximum difference in reactivity is not large considering that some VOCs are calculated to have MIR reactivities greater than 40 times that of ethane, and that the calculated emissions-weighted average MIR reactivity of all VOCs is ~12 times that of ethane on a per gram basis (Carter, 1993a,b).

It is important to recognize that these reactivity calculations for acetone were based on a chemical mechanism for acetone which had not been experimentally verified. The chemical mechanism used to calculate the MIR amd MOIR scales (Carter, 1990) was tested using a variety of smog chamber experiments (Carter and Lurmann, 1991), but only one poorly-characterized outdoor chamber run was relevant for testing the mechanism for acetone, and the mechanism significantly overpredicted the amount of ozone which was formed. No reasonable adjustment of the acetone mechanism within its uncertainty range would permit that acetone experiment to be adequately simulated (unpublished results from this laboratory). Thus the predictions of this mechanism was not consistent with the limited data which was available.

To provide data needed to improve the reliability of assessments of the reactivity of acetone with respect to ozone, the Chemical Manufacturers Association (CMA) contracted us to carry out environmental chamber experiments to measure the incremental reactivity of acetone, to provide data needed to test and improve the reliability of the gas-phase atmospheric chemical mechanism for acetone. A second objective was then to use the experimentally verified mechanism to assess the incremental reactivity of acetone under atmospheric conditions, and in particular its incremental reactivity relative to that of ethane. The results of this study is documented in this report.

Approach

Three types of environmental chamber experiments with acetone were conducted for this study. These are acetone - NO_x experiments, acetone incremental reactivity experiments, and direct acetone vs ethane comparison runs. For comparison and control purposes, we also carried out acetaldehyde - NO_x experiments and incremental reactivity experiments for acetaldehyde, and include in our analysis results of incremental reactivity experiments for ethane which were carried out previously (Carter et al., 1993a). The utility of each are briefly described below.

Acetone - NO_x Experiments

Acetone - NO_x experiments consist of irradiations where acetone is the only reactive organic present in sufficient quantities to significantly affect ozone. In most experiments, low levels (less than ~10 ppb) of tracer species — usually cyclohexane or n-octane — are also present to monitor OH radical levels from their relative rates of decay. These experiments test the acetone mechanism in the absence of complications due to uncertainties in mechanisms for the other VOCs. However, it is not a realistic representation of the chemical environment when acetone reacts in typical ambient atmospheres.

Such experiments do not test the ability of the mechanism to predict the effects of acetone on ozone formation caused by the reactions of the other VOCs present in the atmosphere.

Incremental Reactivity Experiments

Incremental reactivity experiments consist of irradiations of a reactive organic gas (ROG) "surrogate" - NO_x air mixture, alternating (or simultaneously) with irradiations of the same mixture with varying amounts of a test compound such as acetone added. The ROG surrogate - NO_x mixture is designed to approximate the chemical environment in polluted ambient atmospheres, and the irradiation of this mixture without the added test compound is referred to as the "base case" experiment. The experiment where acetone or some other test VOC is added is referred to as the "test" run. The difference between ozone formation and NO oxidation in the test run relative to that in the base case run, divided by the amount of test compound added, is the experimental incremental reactivity. Note that "experimental" incremental reactivity refers to the effect of adding a finite amount of VOC, while incremental reactivity in airshed model calculations refers to the effect of the VOC at the limit as the amount added approaches zero (Carter and Atkinson, 1989). In addition, it should be emphasized that since incremental reactivities are dependent on environmental conditions, and since it is not practical to duplicate in the chamber all the environmental factors which might affect magnitudes of incremental reactivities, incremental reactivities measured in chamber experiments should not be assumed to be quantitatively the same as incremental reactivities in the atmosphere (Carter and Atkinson, 1989). The latter can only be estimated using computer airshed model calculations. The utility of incremental reactivity experiments is that they provide the most direct available means to test of the mechanism's ability to predict incremental reactivities in such calculations.

The "ROG surrogate" is the mixture of reactive organic compounds (ROGs) designed to represent the more complex mixture of ROGs which are present in polluted atmospheres. Three types of ROG surrogates were used in this study: the "mini-surrogate", the "lumped molecule" or "full" surrogate, and the "ethene surrogate". Each have their own sets of advantages and disadvantages, as discussed below.

The Mini-Surrogate is a 3-component mixture consisting of 35% (as carbon) ethene, 50% n-hexane, and 15% m-xylene. This was designed to be an experimentally simple representative of the reactive organic compounds emitted into the atmosphere. Although this mini-surrogate is a significant oversimplification of the complex mixture of ROGs present in the atmosphere (see, for example, Jeffries et al. 1989a), model calculations show that use of this simpler mixture provides a more sensitive measure of reactivities than use of more complex mixtures. In addition to having experimental simplicity while representing the three major classes of emitted hydrocarbons, this surrogate has the advantage of having a large data base of reactivity experiments for other VOCs using this surrogate (see Carter et al, 1993a).

The Full Surrogate is an 8-component mixture which is designed to represent the ROGs present in the atmosphere in as much chemical detail they are represented in the airshed model simulations of their reactions in the atmosphere. Airshed models which represent chemistry at the molecular level [i.e., models other than those using the Carbon Bond mechanisms (Gery et al. 1988)] generally use the following groupings of model species to represent ROG emissions: (1) less reactive alkanes such as n-butane; (2) more reactive alkanes such as n-octane; (3) ethene; (4) terminal alkenes such as propene; (5) internal alkenes such as the 2-butenes; (6) less reactive aromatics such as toluene; (7) more reactive aromatics such as xylenes; (8) formaldehyde; (9) higher aldehydes such as acetaldehyde; and (10) ketones such as methylethyl ketone. Except as indicated below, this surrogate uses a single "real" compound to represent each of these model species. The selected representative compound for each group is generally the one whose mechanism is used to represent that group because it dominates the group or because it is the compound for which there is the most environmental chamber data available to test its mechanism.

Based on the amounts of model species which would be used to represent ambient base ROG mixture utilized to calculate the MIR reactivity scale for the CARB (CARB, 1991; Carter, 1993a,b), the target composition for the full surrogate (as carbon fractions) is: n-butane, 28%; n-octane, 18%; ethene, 27%; propene, 3%; trans-2-butene, 4%; toluene, 9%; m-xylene, 13%; formaldehyde, 1.6%; and 20% inert carbon. (The "inert carbon" is not actually added, but is used when computing the equivalent amount of ambient mixture the surrogate represents.) A separate species is not used for ketones because of their relatively small contribution to the total reactivity of the mixture, and formaldehyde is used to represent all aldehydes in the mixture (on a molar basis) because this substitution simplified the experiments and was calculated not to have a measurable effect on the incremental reactivity results. Thus the 0.8% formaldehyde + 1.5% acetaldehyde carbon is replaced by 1.6% formaldehyde. Model calculations indicate that use of this surrogate in reactivity experiments would give indistinguishable results in reactivity experiments as using full complex ambient mixtures (Carter, 1992). Thus this surrogate has the obvious advantage of being the most realistic, while having the disadvantage of being the most complex to model.

The Ethene surrogate consists of ethene alone. It is designed to be the simplest possible "ROG surrogate" which can be used in reactivity calculations. A simple surrogate is advantageous because its use should introduce the fewest uncertainties when evaluating the ability of a chemical mechanism to predict experimental incremental reactivities. This is because errors in the model for the base ROG surrogate can introduce extraneous or compensating errors in model simulations of experimental reactivity measurements. To be suitable for this purpose, a compound or mixture (1) must have a reasonably well characterized mechanism; (2) must react to form radicals which convert NO to NO_2, (3) must provide internal radical sources which are comparable in magnitude to those from complex mixtures; and (4) should not be completely consumed before the experiment is completed. Ethene appears to be the best candidate in this regard because it has a reasonably well characterized mechanism, has sufficient (but not excessively high) internal radical sources, and because it reacts sufficiently slowly that it is not consumed

during an experiment. In addition, model calculations predict that using ethene as an ROG surrogate would yield almost the same reactivities as using the 3-component mini-surrogate, except under highly NO_x-limited conditions (Carter, 1992).

The incremental reactivity experiments were carried out under NO_x conditions similar to those used to calculate the MIR scale. Thus they are referred to as "maximum reactivity" experiments. These are NO_x conditions where the VOCs have the greatest effect on ozone formation. In addition to providing the most direct test of the ability of a model to predict maximum incremental reactivities, these experiments provide a more sensitive test of the mechanism than experiments with lower NO_x which are less sensitive to the effects of the added VOC. In this study, the NO_x levels employed were ~0.5 ppm. The levels of the base ROG surrogate depended on the surrogate, but were such that ozone formation was still occurring by the end experiments, indicating that NO_x has not been completely consumed.

Acetaldehyde Experiments

For control and comparison purposes, the various types of experiments discussed above were also carried out using acetaldehyde as the test compound. Acetaldehyde is a useful VOC for which to compare the results with acetone because, like acetone, it is photoreactive and forms PAN as the major product in both its OH radical and photolysis reactions (Atkinson, 1990, 1993). It can also be monitored reliably and with reasonably good precision in our experiments. If the model performs as poorly in simulating both acetone and acetaldehyde experiments, it may indicate that the problem is with the base case model or the model for experimental conditions. If, on the other hand, the model performs well in simulating results with one but not the other, it may indicate that problem is with the particular compound which is poorly simulated.

Acetone vs Ethane Reactivity Comparisons

Since one of the objectives of this study is to evaluate whether acetone or ethane forms more ozone in the atmosphere, an obvious type of experiment is to determine the effects of equal amounts of acetone and ethane on ozone formation under the same conditions. However, the effects of VOCs on ozone formation are known to be highly dependent on the conditions in which they react (Dodge, 1984; Carter and Atkinson, 1989; Carter, 1991, 1993a,b; Jeffries and Crouse, 1991). Because of this, if the results of such experiments are to be used to make any conclusions concerning relative reactivities in the atmosphere, the experiments need to duplicate, as closely as possible (and perhaps more closely than practical) the conditions of the atmosphere. Even then, the results would be only applicable to the specific sets of conditions being simulated.

The type of chamber experiment that would most closely duplicate atmospheric conditions would be an incremental reactivity experiment in an outdoor chamber using a fully representative ROG surrogate. Such an experiment was carried using the University of North Carolina dual outdoor chamber (Jeffries,

1993). In that experiment, a mixture consisting of a detailed surrogate + NO_x + an amount of ethane equal to the surrogate on a carbon basis was irradiated simultaneously with equal amounts (on a carbon basis) of surrogate + NO_x + acetone. The run was carried out under low ROG/NO_x conditions. The result was that there was no measurable difference in ozone formation on either side. This might be largely because the amounts of ethane and acetone added were too small to cause a very large effect on the system in the first place, so what was being measured is a difference between two small effects. This run illustrates the small effects both of these compounds have on ozone, and the inconsequential effects of any differences in their reactivities.

Because of the interest expressed by the EPA in this type of experiment (Dimitriades, 1993), we decided to carry out a limited number of such experiments for this program. The main difference is that the ethane and acetone were compared on an equal mass rather than an equal carbon basis, since VOCs are regulated on the basis of mass. The amount of added ethane was such that it had an equal amount of carbons as carbons being represented by the full surrogate (including inert carbons), and the amount of added acetone was such that it had the same mass as the added ethane. Note that because of its greater molecular weight per carbon, the amount of added acetone was 22% lower on a carbon basis than the amount of added ethane.

Experiments with Varying Light Sources

One of the main factors affecting acetone's reactivity is the fact that it undergoes photolysis. Because of this, the nature of the light source used in the environmental chamber experiments will be important. The approach used in this study was to conduct chamber experiments utilizing three different light sources, each with their own unique advantages and disadvantages as discussed below. This provides a much more comprehensive test for the atmospheric reaction mechanism for acetone, and particularly the representation for its photolysis, than would be the case had only a single type of light source been used.

The initial experiments for this study were carried out in chambers employing fluorescent blacklights as the light source. Blacklights have the advantages of being a highly reproducible and easily characterized light source which provides, at relatively low cost, the appropriate light intensity in the UV region where most atmospheric species photolyze. Because of this, it has been utilized as the light source for a large number of environmental chamber experiments which have been used for mechanism evaluation (Carter and Lurmann, 1990, 1991, and references therein), including, most recently, experimental measurements of maximum incremental reactivities of a wide variety of VOCs (Carter et al., 1993a).

Figure 1 shows the solar and blacklight spectra in the wavelength region which affects most photolysis rates in the atmosphere. The action spectra (absorption cross sections x quantum yields) for

NO_2, acetone, and several other representative species are shown for comparison. The light source spectra are all normalized to yield the same NO_2 photolysis rate. While blacklights have the appropriate short wavelength cutoff, it has higher intensity relative to sunlight in the ~330-360 nm region, and much lower intensity at wavelengths greater than ~380 nm, where NO_3 radicals and α-dicarbonyls photolyze. These differences can be corrected for in model simulations of the experiments if the absorption cross sections and quantum yields of the relevant photolyzable species are accurately known.

However, if there are uncertainties in the relevant absorption cross sections or quantum yields, these will be corresponding uncertainties in the ability of the model to appropriately correct for these differences. This is particularly important when evaluating mechanisms for photolyzable species such as acetone. For this reason, several acetone - NO_x, acetone reactivity, and acetaldehyde experiments were carried out in an outdoor chamber using natural sunlight as the light source. Although the representative-ness of the light source is obviously not a problem, the intensity and spectrum changes with time during an experiment, making such experiments more difficult to characterize for quantitative mechanism evaluation purposes. Time-varying temperature also makes such runs more difficult to characterize, especially since some chamber effects are believed to be temperature dependent (Carter and Lurmann, 1990, 1991). Therefore, the evaluation of mechanisms using outdoor chamber data is more qualitative than quantitative. However, if there are major errors in the representation of photolysis reactions in a model which make its predictions grossly inapplicable to atmospheric lighting conditions, they should become apparent when simulating such runs.

Another approach which can be used to evaluate mechanisms for photoreactive species is to conduct indoor chamber experiments using a light source which is more representative of sunlight. This could potentially provide the best features of both indoor and outdoor runs. The best commercially available artificial light source we could find to approximate sunlight is xenon arc lights (Carter and Walters, 1992). As shown on Figure 1, they provide a reasonably good (though not perfect) simulation of sunlight throughout the entire wavelength region where most atmospheric species photolyze. For this reason, we acquired, under DOE funding, a set of xenon arc lights, and constructed an environmental chamber using them. Several acetone - NO_x and acetaldehyde - NO_x runs were conducted using this light source.

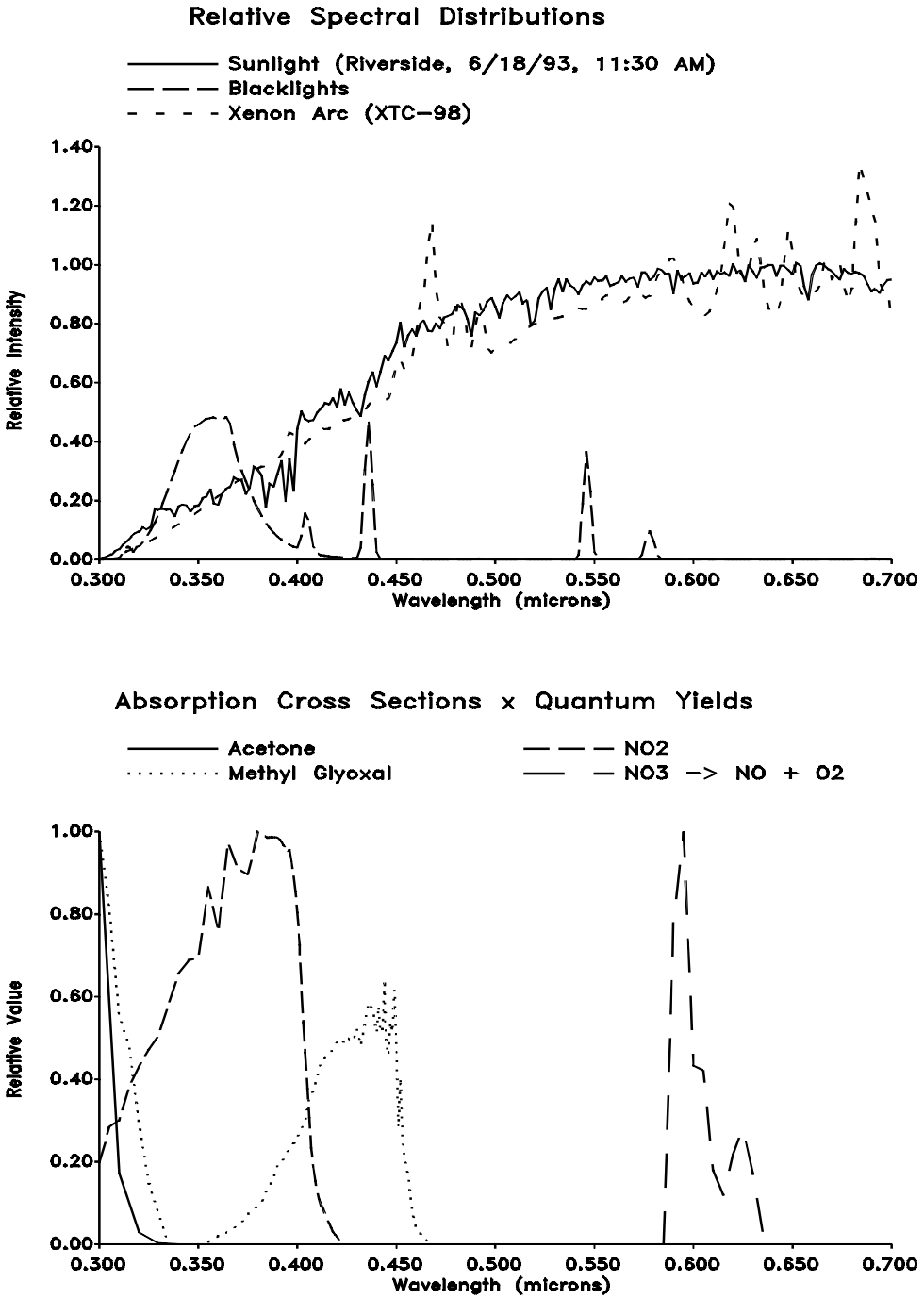

Figure 1. Top Plot shows comparison of spectra of light sources used in the environmental chamber studies. Bottom plot shows spectra of absorption cross sections x quantum yields for selected photoreactive species.

EXPERIMENTAL METHODS

Environmental Chambers

As discussed above, the experiments were carried out using four different environmental chambers using three different types of light sources. These are described in this section.

ETC Blacklight Chamber

This chamber is the same as that utilized in the study documented by Carter et al. (1993a), and is described in greater detail there. It consists of a single ~3000-liter, 2-mil thick FEP Teflon reaction bag fitted inside an aluminum frame with banks of blacklights on the top and bottom, each bank consisting of 30 Sylvania 40-W BL blacklamps. Reflective aluminum paneling is used on all sides. The temperature is controlled by the laboratory air conditioning and fans which exchange the air around the reaction bag with the air in the laboratory. Heaters are used prior to turning the lights on to minimize the temperature rise which occurs when the lights are turned on. For runs prior to ETC-323, dry pure air for the experiments was provided using the SAPRC air purification system which was described in detail previously (Doyle et al., 1977). For subsequent runs, after the chamber was moved to a different location, the dry pure air was supplied using an AADCO air purification system. This AADCO was also used to supply the pure air for the other chambers described below.

DTC Blacklight Chamber (Dividable Teflon Chamber)

This chamber, which was newly constructed during the period of this study for use in place of the ETC, is actually two adjacent chambers which can be operated simultaneously using the same light source and temperature control system. These are referred to as the two "sides" of the chamber (Side A and Side B) in the discussion of the results. The DTC consists of two 4600-liter 8’ x 6’ x 4’ 2-mil thick FEP Teflon reaction bags in an 8’ x 8’ chamber enclosure room. The bags are interconnected with two ports each with Teflon-coated fans and blowers which rapidly exchange their contents to assure that reactants which are desired to have equal concentrations in each are equalized. The fans also mix the contents within each chamber. The ports can then be closed to allow separate injections on each side, and separate monitoring of each. The chamber enclosure room has two banks of blacklights on opposing walls, with polished aluminum reflective material on the other walls and floor, and with perforated aluminum reflective material on the ceiling, through which cooling air can be forced. Specially constructed shaped aluminized plastic reflectors are used for the blacklights. The lighting system was found to provide so much intensity that only half the lights were used in these runs. A thermostatted temperature control system controlling a dedicated air conditioner for the chamber enclosure maintains the temperature to within ±1˚ C and minimizes the sudden temperature rise which would otherwise occur when the lights are turned on. The AADCO air purification system supplies pure dry air for this chamber.

This chamber would be expected to provide similar types of data as the ETC because it is constructed of the same material, utilizes the same type of lights, and has approximately the same light intensity. However, its dual chamber construction is particularly well suited for reactivity experiments, with the base case irradiation being conducted simultaneously with the added test compound experiment utilizing the same initial base case reactant concentrations and the same temperature profile and light intensity. Alternatively, two different experiments can be conducted simultaneously.

Outdoor Teflon Chamber (OTC)

The SAPRC OTC, which has been described in detail elsewhere (Carter et al., 1984, 1986), consists of a ~30,000-50,000-liter, 2-mil thick FEP Teflon, pillow-shaped reaction bag located outdoors. The reaction bag is supported by nylon ropes on a framework and held 2.5 feet off the ground to allow air circulation under the chamber. A green indoor-outdoor carpet is located under the chamber. When the chamber contents are not being irradiated, the reaction bag is covered by an opaque, grey trap attached to a dual framework of steel tubing which can be readily opened to uncover the chamber and initiate the irradiation. The AADCO air purification system supplies pure dry air for this chamber.

This chamber can be operated in a dual mode to allow two parallel experiments under the same lighting and temperature conditions. This division of the chamber into two separate reactors, which can be accomplished after reactants common to both chamber sides are injected and mixed, is accomplished by means of three 1 1/4-in diameter cast-iron pipes, which are surrounded by foam to protect the Teflon reactor. The reaction bag is divided by raising the lower pipe and placing it tightly between the upper pipes, then rotating them by 180 degrees. Previous tests have shown that this forms a tight seal, with the exchange between the chamber sides being less than 0.1% per hour (Carter et al., 1981). The chamber is oriented such that the pipes dividing the chamber run in a north-south direction, with side A, by convention, always being on the eastern half of the chamber. All OTC experiments discussed here were conducted with the chamber in the divided mode.

Xenon Teflon Chamber (XTC)

This chamber, which was completed near the end of the time period of this study, is similar in size and construction of one of the DTC chambers, but differs in the nature of the light source. The XTC consists of a ~5200-liter, 6’ x 8’ x 4’ 2-mil thick FEP Teflon reaction bag located on one end of a 8’ x 10’ chamber enclosure with reflective walls, floor and ceiling, and has a set of four Atlas RM-65A 6.5 kw Xenon arc lights mounted on the opposite wall. The design objectives for this chamber and lighting system is described elsewhere (Carter and Walters, 1992). It actually uses the same enclosure as the DTC chambers, but in a different configuration. The side walls are the molded aluminized plastic reflectors for the blacklights used for the DTC, with the blacklights removed. Sliding aluminum paneling are used to prevent the Xenon lights from irradiating the chamber when they are being turned on and stabilizing. AADCO air purification system supplies pure dry air for this chamber.

Experimental Procedures and Analytical Methods

The chambers were flushed with dry purified air for 6-9 hours on the nights before the experiments. The monitors were connected prior to reactant injection and the data system began logging data from the continuous monitoring systems. The reactants were injected as described previously (Carter et al, 1993a). For dual chamber (DTC or OTC) runs, the common reactants were injected in both sides simultaneously (using a "T" in the injection line) and were well mixed before the chamber was divided. In the case of the OTC, the reactants were mixed by manual agitation of the reaction bag, while with the DTC the contents of side A were blown into side B and vise-versa using two separate blowers. Fans were used to mix the reactants in the indoor chambers during the injection period, but these were turned off prior to the irradiation. Dividing the OTC consisted of clamping the reaction bag in two using pipes, while "dividing" the DTC consisted of closing the ports which connected the two reaction sides. After the OTC or DTC were divided, the reactants for specific sides were injected and mixed. The irradiation began by turning on the lights (for the blacklight chambers), opening the cover (for the OTC), or slighting back the panels in front of the Xenon lights (which were turned on ~30 minutes previously). The irradiation proceeded for 6 hours. After the run, the contents of the chamber(s) were emptied (by allowing the bag to collapse) and flushed with purified air.

Ozone and nitrogen oxides were continuously monitored using commercially available continuous analyzers with Teflon and borosilicate glass sample lines inserted directly into the chambers (ca 18 in.). For DTC and OTC chamber runs, the sampling lines from each half of the chamber were connected to solenoids which switched from side to side every 10 minutes, so the instruments alternately collected data from each side. Ozone was monitored using a Dasibi Model 1003AH UV photometric ozone analyzer and NO and total oxides of nitrogen (including HNO_3 and organic nitrates) were monitored using either a Columbia Model 1600 or a Teco Model 14B or 43 chemiluminescent NO/NO_x monitor. The output of these instruments, along with that from the temperature and (for OTC and XTC runs) light sensors were attached to a computer data acquisition system, which recorded the data at periodical intervals, using 30 second averaging times. For single mode (ETC or XTC) chamber runs, the O_3, NO_x, and other continuous data recorded every 15 minutes; for the divided chamber (DTC or OTC) runs, the data was collected every 10 minutes, yielding a sampling interval of 20 minutes for taking data from each side.

Organic reactants other than formaldehyde were measured by gas chromatography with FID detection as described elsewhere (Carter et al., 1993a). GC samples were taken for analysis at intervals from fifteen minutes to one hour using 100 ml gas-tight glass syringes. These samples were taken from ports directly connected to the chamber. The syringes were flushed with the chamber contents several times before taking the sample for analysis.

Formaldehyde was monitored using a diffusion scrubber system based on the design of Dasgupta and co-workers (Dasgupta et al, 1988, 1990; Dong and Dasgupta, 1987), as described elsewhere (Carter

et al., 1993a). This system alternately collected data in sample (30 minutes), zero (15 minutes), and calibrate mode (15 minutes), for a one hour cycle time. The readings at the end of the time period for each mode, averaged for 30 seconds, were recorded on the computer data acquisition system, which subsequently processed the data to apply the calibration and zero corrections. A separate sampling line from the chamber was used for the formaldehyde analysis. For the DTC or OTC, a solenoid, which was separate from the one used for O_3 and NO_x sampling, was used to select the chamber side from which the formaldehyde sample was withdrawn, which alternated every 15 minutes. This yielded formaldehyde data as frequently as every 15 minutes for single chamber (ETC and XTC) runs, and every 30 minutes for each side of DTC and OTC runs.

Characterization Methods

Temperature

For the blacklight chambers, the temperature was monitored using an unshielded thermocouple inside the chamber. Subsequent comparison of temperatures monitored with this method with simultaneous readings using the aspirated temperature probe (discussed below) gave results which were within ±0.2°C, indicating that heating of the thermocouple by the light from the blacklights is small. This is expected because of the low visible and infrared energy of those lights. The temperature in the ETC and DTC runs were typically 26-30˚C.

Prior to run XTC-090 the temperature was monitored in the XTC chamber using a thermocouple inside the chamber shielded by a piece of reflective aluminum. During that period temperature probes were also located in the formaldehyde and NO_x/O_3 sampling lines, but these data were not considered to be as reliable because the sensors were outside the chamber. Although the temperature readings in the sample lines were higher than the temperature in the laboratory, they tended to decrease with time during the run, while the probes inside the chamber indicated that the temperature was increasing slightly. Following run XTC-090, the temperature was monitored with the thermocouple inside an opaque 1/4" OD sample line inside the chamber, with air being drawn through at a rate of 2 l/min. This is referred to as the aspirated temperature probe. Provided that the flow rate past the sensor is sufficient, this method is considered to give the more accurate temperature reading. Tests showed that a flow rate of be at least 2 l/min was required for the measured temperature to be independent of the flow. Comparison of the data taken simultaneously indicated that the shielded probe in the chamber gave readings which were ~1.5˚C higher than the aspirated shielded probe.

Except for run XTC-083, the temperatures monitored during XTC runs were highly consistent, increasing rapidly from room temperature to 28-30° C immediately after the lights are turned on, to 29-31° C by the end of the runs. For some reason, the temperature probe in the chamber gave readings which were ~2 degrees higher for run XTC-083, though separate temperature probes in the sampling lines indicated no differences between the temperature in that run and the others. For that reason, and the fact

that the temperatures were consistent from run to run for the other runs, we believe that the measured readings were probably unreliable for that run.

An analogous change in temperature monitoring method was made for the outdoor chamber experiments. For the runs in 1992 (run OTC-270 and earlier), temperature was monitored using unshielded probes inside each chamber side, while for the other runs reported here (Runs OTC-271 and later) temperature was monitored by shielded probes in the sample line, located slightly outside and underneath the chamber.

Light Intensity and Spectra

The light intensity in the ETC and DTC was monitored by periodic NO_2 actinometry experiments utilizing the quartz tube method of Zafonte et al (1977), with the data analysis method modified as discussed by Carter et al. (1993a). The measurements were made either with the quartz tube in the reaction bag or with a Teflon film sleeve around the tube so the results would incorporate the effect of the light passing through the chamber walls. Based on the results of these runs, the NO_2 photolysis rate associated with the blacklight chamber runs were as follows:

- ETC-243 through ETC-247 and associated base case runs: 0.32 ± 0.02 min^{-1}.
- ETC-445: 0.336 ± 0.012 min^{-1}.
- All DTC runs: 0.38 ± 0.02 min^{-1}.

The relative spectral distributions of the blacklight light sources were measured using a LiCor LI-1800 portable spectrometer. The spectrum did not vary significantly with the chamber used or the age of the lights, and the spectra taken using the LiCor using these chambers were essentially the same as spectra of the lights in the SAPRC ITC chamber using a different spectrometer (Carter et al., 1984).

The light characterization for the XTC chamber was similar to that for the blacklight chambers, with the absolute intensity being determined by NO_2 actinometry using the quartz tube method, and the relative spectra being determined by measurements using the Li-1800 spectrometer. However, the spectra of xenon arc lights are expected to change gradually as the lights age, so spectra were taken 3-4 times during each XTC run.

The NO_2 photolysis rates measured by actinometry inside the XTC chamber was found to be 0.24-0.26 min^{-1} after the lights were first installed (run XTC-79), and declined to a constant value of 0.23 min^{-1} in subsequent determinations (runs XTC-89 and XTC-100). The relative change in NO_2 photolysis rate with time during the experiments could also be obtained from the absolute light intensities measured by the LiCor spectrometer. These data indicated that the NO_2 photolysis rates declined by ~3% between runs XTC-80 and around XTC-85, and was essentially constant after that. Based on the precision of the initial actinometry results, the NO_2 photolysis rates measured in the XTC are estimated to be uncertain by ~5%.

The sunlight intensity for the outdoor chamber runs was monitored continuously using an Eppley UV radiometer and an Eppley PSP total broadband radiometer, and the global and diffuse light spectra were measured approximately hourly during the runs using the LiCor spectrometer. The global spectrum is that obtained with the unshaded instrument, while the diffuse spectrum is that obtained by shading the sensor with a 10.0 cm disk held 90 cm from the sensor, positioned so that the shadow of the disk covers the sensor (Jeffries, personal communication; Jeffries et al., 1989b). These data were used as input to a light model, discussed later in this report, to calculate light intensity and spectra as a function of time during the runs.

Dilution

Dilution due to sampling is expected to be small because the flexible reaction bags can collapse as sample is withdrawn for analysis. However, some dilution occasionally occurs because of small leaks, and several XTC runs had larger than usual dilution due to a larger leak which was subsequently found and repaired. Information concerning dilution in an experiment can be obtained from relative rates of decay of added VOCs which react with OH radicals with differing rate constants (Carter et al., 1993a). All experiments had a more reactive compound (such as m-xylene or n-octane) present either as a reactant or added in trace amounts to monitor OH radical levels. Trace amounts (~0.1 ppm) of n-butane was added to experiments if needed to provide a less reactive compound for the purposes of monitoring dilution. In many experiments, dilution rates were zero within the uncertainties of the determinations.

Control Experiments

Several types of control experiments were conducted to characterize chamber conditions. Ozone decay rate measurements were conducted with new reactors, and the results were generally consistent with ozone decays observed in other Teflon bag reactors (Carter et. al. 1984, 1986). NO_x-air irradiations with trace amounts of propene or isobutene, or n-butane-NO_x-air experiments, were conducted to characterize the chamber radical source (Carter et al., 1982).

Reactivity Data Analysis Methods

As described above, reactivity experiments consist of one or more "base case" run(s) combined with a "test" experiment in which a VOC is added to the base case reactants. The results of these experiments can be analyzed to yield several measures of VOC reactivity (Carter et al., 1993a,b), though in this report we will focus on the effect of the VOC on the amount of NO reacted plus the amount of ozone formed at hourly intervals in the experiment. This is abbreviated as d(O_3-NO) in the subsequent discussion. As discussed elsewhere (e.g., Johnson, 1983; Carter and Atkinson, 1987; Carter and Lurmann, 1990, 1991) this gives a direct measure of the amount of conversion of NO to NO_2 by peroxy radicals formed in the photooxidation reactions, which is the process that is directly responsible for ozone

formation in the atmosphere. The incremental reactivity of the test VOC relative to $d(O_3\text{-NO})$ at time t, designated $IR[d(O_3\text{-NO})]_t^{voc}$, is given by

$$IR[d(O_3\text{-NO})]_t^{voc} = \frac{d(O_3\text{-NO})_t^{test} - d(O_3\text{-NO})_t^{base}}{[VOC]_0}$$

where $d(O_3\text{-NO})_t^{test}$ is the $d(O_3\text{-NO})$ measured at time t from the experiment where the test compound (e.g., acetone) was added, $d(O_3\text{-NO})_t^{base}$ is the corresponding value from the base case experiments where the test VOC was not present, and $[VOC]_0$ is the amount of test VOC added. The incremental reactivity with respect to $d(O_3\text{-NO})$ was calculated for each hour of the experiment.

The quantities $d(O_3\text{-NO})^{test}$ and $[VOC]_0$ are obtained from the results of each of the individual test experiments. The methods used to derive $d(O_3\text{-NO})^{base}$ depended on whether the base case experiment was being carried out at the same time under the same conditions in a divided or double chamber, as is the case with DTC or OTC runs, or whether the base case experiment was carried out separately, as was the case with the runs in the ETC. In the former case, the data from the base case side irradiated simultaneously with the test run was used. In the ETC experiments, the effects of run-to-run variability in temperature, light intensity, and initial reactant concentrations on $d(O_3\text{-NO})$ had to be taken into account. For these runs, the base case results used in the reactivity analysis of a particular test run were derived from estimates, based on a linear regression analysis of results of many base case runs, of what the result of a base case experiment would be if it were carried out with the same temperature, light intensity, and initial base case reactant concentrations as the test run. The methods and data used in the analysis of the ETC reactivity experiments are described in detail elsewhere (Carter et al., 1993a).

MODEL SIMULATION METHODS

Computer model simulations were conducted to evaluate the extent to which the results of these experiments are consistent with predictions of a current chemical mechanism for the atmospheric reactions of acetone and other VOCs. The mechanism was then used to simulate the incremental reactivities of acetone, ethane, and other VOCs under atmospheric conditions. The following sections give descriptions of the chemical mechanisms employed, of the methods used when simulating the chamber experiments, and of the model and scenarios used when simulating atmospheric reactivities. The chemical mechanism was updated for the purpose of this study. The overall mechanism used for all the atmospheric species is described first, followed by a more detailed discussion of the mechanism used for acetone.

General Atmospheric Mechanism

The chemical mechanism used as the starting point for this study is the "SAPRC-90" mechanism as documented by Carter (1990), with updates for various VOCs made in conjunction with its use to calculate the MIR scale for the California ARB (Carter, 1993a). This mechanism was then updated further before use in this study, as discussed below. These updates take into account results of several recent laboratory studies and incorporate some of the major recommendations made by Gery (1991) in his review of the SAPRC-90 mechanism. The specific changes in the mechanism, relative to the SAPRC-90 mechanism used in the MIR calculation (Carter, 1993a,b), are as follows:

(1) The formaldehyde absorption cross-sections were updated based on the recent data of Cantrell et al. (1990) and Rogers (1989). This results in a slight increase in the formaldehyde photolysis rate.

(2) The kinetics for the reactions of the acetyl peroxy radical with NO and NO_2, which are involved in the formation and decomposition of PAN, and the kinetics of the thermal decomposition of PAN, were updated based on recent experimental results of Tuazon et al. (1991) and Bridier et al. (1991). This causes the model to predict somewhat higher ozone formation rates than the SAPRC-90 mechanism.

(3) The SAPRC-90 mechanism uses model species whose photolysis rates are adjusted to fit aromatic-NO_x-air chamber experiments to represent the unknown photoreactive aromatic fragmentation products (Carter, 1990). This approach is still used in the updated mechanism, except that the change in the acetyl peroxy and PAN kinetics required reoptimization of these photolysis rates. In addition, the action spectra (absorption coefficients x quantum yields) for these products were assumed to proportional for the absorption cross section for acrolein (Gardner et al., 1987), rather than using the somewhat arbitrary action spectrum in the SAPRC-90 mechanism. These changes were found not to significantly

affect the performance of the mechanism if the reoptimization is conducted using the same set of experiments as used in the development of SAPRC-90.

(4) The mechanisms for the reactions of ozone with alkenes were modified to be consistent with the data of Atkinson and Aschmann (1993), who observed much higher yields of OH radicals than predicted by the SAPRC-90 mechanism. To account for these data, it was assumed that (1) the formation of OH radicals dominates over other radical-forming fragmentation processes, and (2) in the reactions of unsymmetrical alkenes, the more substituted Criegee biradical, which forms higher OH yields, are formed in relatively higher yields than the less substituted biradicals. The modified ozone reactions for the alkenes discussed in this paper are:

$$\text{Ethene} + O_3 \rightarrow HCHO + (HCHO2)$$
$$\text{Propene} + O_3 \rightarrow 0.6\ HCHO + 0.4\ CCHO + 0.4\ (HCHO2) + 0.6\ (CCHO2)$$
$$\underline{\text{trans}}\text{-2-Butene} + O_3 \rightarrow CCHO + (CCHO2)$$
$$\text{Isobutene} + O_3 \rightarrow 0.82\ HCHO + 0.18\ ACET + 0.18\ (HCHO2) + 0.82\ (C(C)CO2)$$

where CCHO and ACET represent acetaldehyde and acetone, and (HCHO2), etc., represent the excited Criegee biradicals, which are represented as reacting as follows:

$$(HCHO2) \xrightarrow{fast} 0.12\ CO + 0.12\ HO. + 0.12\ HO2. + 0.88\ (\text{unreactive carbon})$$

$$(CCHO2) \xrightarrow{fast} 0.3\ HCHO + 0.3\ CO + 0.6\ HO. + 0.3\ \{CCO\text{-}O2.+\ RCO3.\} + 0.3\ \{RO2\text{-}R.+\ RO2.\} + 0.9\ (\text{unreactive carbon})$$

$$(C(C)CO2) \xrightarrow{fast} HCHO + HO. + \{R2O2.+\ RO2.\} + \{CCO\text{-}O2.+\ RCO3.\}$$

[See Carter (1990) for a description of the model species and the methods used to represent peroxy radical reactions.] This is clearly an oversimplification of this complex system (e.g., see Atkinson, 1990, 1993), but is intended to account for the observed OH radical yields and represent the major features affecting these compounds' reactivities. Note that this new mechanism gives substantially higher radical yields in the ozone + alkene systems than the SAPRC-90 mechanism, particularly for internal alkenes.

(5) The reaction of NO with the peroxy radical formed in the reaction of OH radicals with isobutene was assumed to form the corresponding hydroxyalkyl nitrate 10% of the time. This assumption resulted in significant improvements to the fit of model simulations to ozone and PAN yields in isobutene - NO_x - air chamber experiments. Without this assumption, the model with the OH yields indicated by the O_3 + isobutene data of Atkinson and Aschmann (1993) significantly overpredicts O_3 formation rates. If lower radical yields in the O_3 + isobutene reaction are assumed, the model significantly underpredicts PAN (unpublished results from this laboratory).

(6) The representation of isooctane was modified to improve the model simulations of its reactivity (Carter et al., 1993a,b).

(7) Several changes were made to the mechanism for acetone. These are discussed in the following section.

A complete listing of this mechanism as used in the model simulations in this report is given in Appendix A. Further updates to this mechanism are planned and it has not been as extensively evaluated against the chamber data as the SAPRC-90 mechanism (Carter and Lurmann, 1991). However, it was evaluated in model simulations of the results of the extensive set of maximum incremental reactivity experiments recently completed in our laboratories (Carter et al, 1993a), and was found to perform somewhat better than the SAPRC-90 mechanism in simulating these data.

Acetone Mechanism

Acetone is believed to react in the atmosphere primarily by photolysis and reaction with OH radicals, and the available data concerning these reactions are discussed by Atkinson (1990, 1993). Reaction with ozone would be expected to be of negligible importance (Atkinson and Carter, 1984), and although there are no data available concerning its reaction with NO_3 radicals, the rate constant would be expected to be small (Atkinson, 1991). The mechanisms used in the model to represent the OH and photolysis reactions are discussed below.

OH Radical Reaction

The representation of the OH + acetone used in the SAPRC-90 mechanism is based on the recommendations of Atkinson (1990). The recommended rate constant expression is equivalent to $k = 1.92 \times 10^{-13} (T/300)^2 e^{0.11/RT}$ cm^3 $molec^{-1}$ sec^{-1}, which yields $k = 2.31 \times 10^{-13}$ cm^3 $molec^{-1}$ sec^{-1} at 300K. The reaction is assumed to proceed as follows:

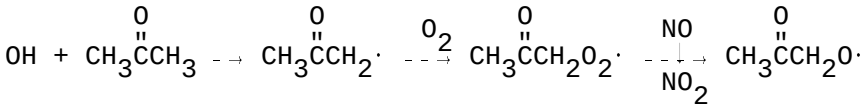

The alkoxy radical can either react with OH radicals, giving rise to methylglyoxal,

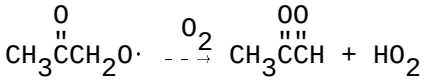

(a)

or it undergo decomposition, giving rise to methylperoxy or acetylperoxy radicals, which react further to ultimately form either formaldehyde + PAN or two formaldehyde + CO_2, depending on the $[NO]/[NO_2]$ ratio.

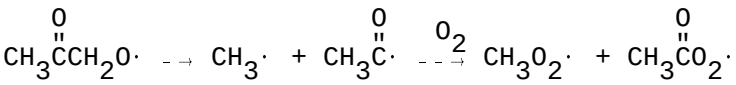

(b)

At the time the SAPRC-90 mechanism was developed, there was no experimental information available concerning the mechanism for this reaction, or the k_a/k_b branching ratio. This could be an important factor affecting acetone's reactivity because methylglyoxal is a highly photoreactive product whose formation in the mechanism would enhance acetone predicted reactivity, while PAN formation is a radical termination process whose formation would have an inhibiting effect. Based on an estimate given by Atkinson (1990), the SAPRC-90 mechanism assumes that methylglyoxal formation occurs 80% of the time, i.e., that $k_a/k_b = 4$.

However, more recent data and evaluations indicate that modifications to this OH + acetone mechanism are appropriate. In an updated evaluation, Atkinson (1993) gives a slightly different recommended rate constant expression for this reaction. The new recommendation is equivalent to $k = 4.81 \times 10^{-13} (T/300)^2 e^{-0.457/RT}$ cm^3 $molec^{-1}$ sec^{-1}, which yields $k = 2.23 \times 10^{-13}$ cm^3 $molec^{-1}$ sec^{-1} at 300 K. Although this gives essentially the same rate constants for the temperature range of these experiments, the mechanism used in this study was updated to be consistent with this new recommendation.

More significantly in terms of predictions of acetone's reactivity, recent data from Jenkin et al (1993) indicate that reaction of the $CH_3COCH_2O_2\cdot$ radical to form methylglyoxal is not important. This is consistent with predictions of a revised estimation technique developed by Atkinson and Carter (1992) based on recent data concerning decomposition and O_2 reactions of analogous reactions of alkoxy radicals formed from ethers and other compounds. Based on this, the updated OH + acetone mechanism used in this study assumes that reaction (b) is the only significant process, and that methylglyoxal formation is negligible. This results in a mechanism which predicts somewhat lower reactivity for acetone than does SAPRC-90.

Photolysis Reaction

Available data concerning the photolysis of acetone under atmospheric conditions are summarized in the latest IUPAC evaluation (Atkinson et al., 1992). The recommended absorption cross sections and quantum yields are those of Meyrahn et al. (1986), while the SAPRC-90 mechanism (Carter, 1990) uses values from Calvert and Pitts (1966). The latter agree with the recommended values at wavelengths greater than 310 nm, but are slightly lower at lower wavelengths, though the difference causes only a ~1.5% change in the calculated atmospheric photolysis rate. Nevertheless, the updated mechanism was modified to incorporate the recommended absorption cross sections.

The only energetically available photodecomposition reaction for acetone at wavelengths greater than 300 nm is scission of the C-CO bond, forming, in the presence of oxygen, methylperoxy and acetyl-peroxy radicals

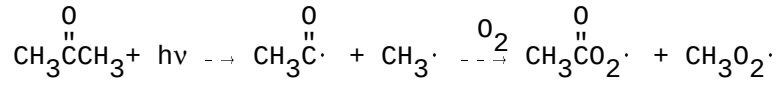

In the presence of NO_2 acetylperoxy radicals subsequently react to form PAN. There is disagreement in the literature concerning the quantum yields for this reaction under atmospheric conditions. Gardner et al. (1984) derived quantum yields of 0.07, approximately independent of wavelength over the 280-313 nm region, based on acetone loss and yields of CO_2, CO, CH_3OH, and formaldehyde products when acetone was photolyzed in air. Meyrahn et al. (1986) derived quantum yields which generally decreased wavelength from 250-330 nm based on measuring yields of PAN in photolyses of ~150 ppm of acetone and ~0.12 ppm of NO_2 in air. The IUPAC panel recommends use of the data of Meyrahn et al (1986) because they appeared to the evaluators to be more reasonable (Atkinson et al., 1992). These recommended absorption cross sections were used in the SAPRC-90 mechanism.

The validity of the quantum yields reported by Meyrahn et al (1986) is based on the assumption that under the conditions of their experiments all the acetyl peroxy radicals formed react to form PAN, and that there is no other source of these radicals. However, as discussed in the previous section, the OH reaction is also believed to form these radicals, and if sufficient OH were present in their experiments, there could be an additional source of PAN from the this reaction and the reported quantum yields may be high. To examine this, the conditions of these experiments were modeled using the updated SAPRC-90 mechanism. The model simulations predicted that the OH reaction was negligible in the experiments carried out at wavelengths of 310 nm or less, but that this reaction forms ~10% of the PAN in the experiments at 320 nm and ~50% of the PAN at 330 nm. This can be corrected for (albeit approximately) by reducing the 320 nm quantum yields by 10% (from 0.028 to 0.026) and the 330 nm quantum yields by a factor of ~2 (from 0.033 to 0.017). The corrections, particularly at 330 nm, must be considered to be highly approximate because we probably did not simulate the conditions of the experiments exactly. However, the factor of two correction of the 330 nm quantum yield gives a more reasonable decline in quantum yields with wavelength than the uncorrected data, so the updated mechanism incorporated these corrections to the Meyrahn et al. (1986) quantum yields. This correction causes a ~4% reduction of the atmospheric photolysis rate for acetone.

The model simulations of the experiments at wavelengths of 310 nm or less predict that not all the of the acetylperoxy radicals react to form PAN, since some will be lost by various peroxy + peroxy radical reactions. The model simulations we conducted suggested that the PAN yields in those experiments may underestimate the true quantum yields by ~15-20%. This would result in comparable increases of the calculated atmospheric photolysis rates for acetone, since this wavelength region accounts

for most of the photolysis reaction. These estimates are uncertain because the predicted extent of peroxy + peroxy reaction is dependent on our model for the conditions of these experiments, whose accuracy is unknown. The underprediction of quantum yields could be no more than ~20%, since otherwise the corrected quantum yields for 250 - 260 nm would be greater than unity. For this reason, no such correction to the $\lambda < 210$ nm quantum yields were applied. However, this analysis indicates that the quantum yields which are up to ~20% higher than assumed in the model may not necessarily be inconsistent with the data of Meyrahn et al (1986).

Because of the disagreement in the literature, the quantum yields for acetone photolysis must be considered the most uncertain component of acetone's atmospheric photooxidation mechanism. If the quantum yields reported by Gardner et al. (1984) are assumed, the acetone photolysis rate is calculated to be ~45% higher in the atmosphere and ~2 times higher in a blacklight chamber experiment, than calculated using the corrected data of Meyrahn et al. (1986). Given the complexity of the chemical systems utilized in both these studies, and the assumptions concerning the mechanisms that need to be made in analyzing the results, the possibility that neither of these determinations are correct cannot be ruled out.

Several adjustments were made to the assumed acetone quantum yields, and their wavelength dependencies, to improve the fits of the model simulations to the experiments carried out in this study. These are discussed in the Results section.

Model Simulations of Chamber Experiments

The testing of a chemical mechanism against environmental chamber results requires that the model include appropriate representations for chamber-dependent effects such as wall reactions and characteristics of the light source used during the experiments. The methods used to represent them in this study are based on those discussed in detail by Carter and Lurmann (1991), adapted for these specific sets of experiments as discussed by Carter et al. (1993a) or as indicated below. Where possible, the parameters were derived based on analysis of results of characterization experiments carried out in conjunction with these runs.

Light Characterization for Indoor Chamber Runs

Light characterization for indoor chamber runs consist of NO_2 actinometry experiments and measurements of the spectrum of the light source using the LI-1800 spectrometer. The former give the absolute light intensities in terms of the NO_2 photolysis rates, while the latter give information needed to calculate the ratios of rates of all other photolysis reactions to that for NO_2, given the absorption cross sections and quantum yields for the NO_2 and other photolysis reactions. In particular, the relative spectral measurements are converted to absolute actinic fluxes by multiplying them by a factor which, when used with the currently accepted NO_2 absorption cross sections and quantum yields (Atkinson, 1990; Carter,

1990), result in the calculated NO_2 photolysis rate being equal to the value derived from the actinometry experiments. The absolute actinic fluxes are then used to calculate the rates of all the other photolysis reactions in the model simulations.

This procedure uses the data from the actinometry experiments to give the absolute light intensities, with the LI-1800 spectrometer only being used to obtain relative spectra. However, the LI-1800 spectrometer is calibrated at the factory to give absolute light intensity readings, and thus, in theory at least, it could be used to as a means to assess the accuracy of the actinometry experiments. Unfortunately, the spectrometer measures light intensity on a plane, while photolysis rates are determined by spherically integrated light intensities. To determine the latter from the former, and thus provide an independent check of the accuracy of our actinometry measurements, we developed a model for the special distribution of the light in the chamber, making measurements to estimate reflectances within the chamber (unpublished results from this laboratory). The NO_2 photolysis rate derived from this procedure was found to be ~10% lower than that measured using the quartz tube actinometer. This is considered to be agreement to within the uncertainties of the model and the measurements, and thus a validation of our NO_2 actinometry method.

The spectra for the blacklight chambers were found to be essentially independent of chamber and lamp age, at least in the wavelength region which affects photolysis rates. Thus the same spectrum was used in the model simulations of these runs. However, the spectrum of the xenon arc light source used in the XTC runs was found to change slowly with time, becoming somewhat weaker in the shortest wavelengths as the lamps aged. The affected wavelengths were shorter than those which significantly influence NO_2 photolysis rates, and the intensity of the spectra indicated that NO_2 photolysis rates decreased by only ~3% during the course of this study. On the other hand, the photolysis of other species, including acetone, are more affected by this change. For example, between runs XTC-80 and XTC-98 the photolysis rate of acetone, relative to that for NO_2 was calculated to decline by ~14%. Because of this, photolysis rates were calculated separately for each XTC run. Based on the results of the actinometry experiments, combined with the monitoring of the light intensity with the spectrometer, we assign an NO_2 photolysis rate of 0.24 min^{-1} for run XTC-80, 0.23 for run XTC-85 and those following, and intermediate values for runs between XTC-80 and XTC-85. The photolysis rates for the other reactions were calculated using the relative spectra measured during each individual run.

Light Characterization for Outdoor Chamber Runs

The light characterization data for the outdoor chamber runs consist of continuous UV and broadband radiometer data, and approximately hourly global and diffuse solar spectra taken using the LI-1800 spectrometer. The global and diffuse spectra, along with the JSPECTRA solar light model developed by Jeffries (1988, 1989b, 1991), were used as the primary means for light characterization for modeling purposes. The procedure employed is only applicable to clear sky conditions, so no runs on

cloudy or overcast days were used for mechanism evaluation. The radiometer data was used as a cross-check to assure that the light conditions were not changing abruptly between the times spectral measurements were made. The outdoor chamber light characterization procedures will be documented in a subsequent report, and will only be summarized here.

The JSPECTRA solar light model is designed to calculate ground-level solar spectra given relevant parameters such as time of day, day of year, total ozone column, atmospheric aerosol parameters, and extraterrestrial solar fluxes. It can be used either to calculate spherically integrated actinic fluxes for calculation of photolysis rates or to predict global or diffuse spectra as measured by the LiCor spectrometer. Some of the inputs to the program, such as the time of day or day of year, are known, others, such as the extraterrestrial fluxes, are assumed not to be variable and are provided with the program, while other inputs, such as the ozone column and the aerosol parameters, are uncertain or variable. The most sensitive of the uncertain inputs were adjusted, using a non-linear optimization algorithm, to fit the global and diffuse LiCor spectra taken during the run, while for the less sensitive parameters the defaults used by Jeffries (1988) for "summer conditions" were used in all calculations. Although moderately good fits of adjusted model calculation to LiCor spectra could obtained by adjusting only the parameters in the JSPECTRA model, for best fits to the data three separate parameters were added to scale the overall intensity as a function of wavelength. These consisted of scaling factors for the intensities at 300, 500, and 800 nm; the scaling factors for other wavelengths were obtained by linear interpolation of these. With the set of parameters we used, these scaling factors were consistently 0.7, 1, and 1.1 at these three wavelengths, respectively. An example showing the comparison obtained between the adjusted model calculation and the global and diffuse LiCor spectra is shown on Figure 2

The results of the optimization of the JSPECTRA input parameters could then be used to calculate spherically integrated actinic fluxes for the times the LiCor spectra were taken. The calculated spherically integrated fluxes were not sensitive to the specific set of JSPECTRA parameters optimized, as long as the model could closely simulate the direct and diffuse LiCor data. If the run was carried out on a clear day, the parameters affecting light fluxes might reasonably be assumed not to change abruptly with time. In this case, the values of the adjusted parameters for times between those where LiCor data were taken could be estimated by linear interpolation of the optimized values. Based on this assumption, parameters were estimated at each 20 minute interval during the run, from which actinic fluxes for those times were calculated. The fact that this assumption is not valid for cloudy days is not a significant limitation because the JSPECTRA model was not designed to calculate solar fluxes for those conditions in any case. For this reason, only data from clear day runs were characterized for modeling purposes. The few runs carried out on days with unfavorable weather are not discussed.

The JSPECTRA program, with its time-varying inputs derived as discussed above, could also be used to calculate how the data from the UV and broadband radiometers should vary with time. Thus,

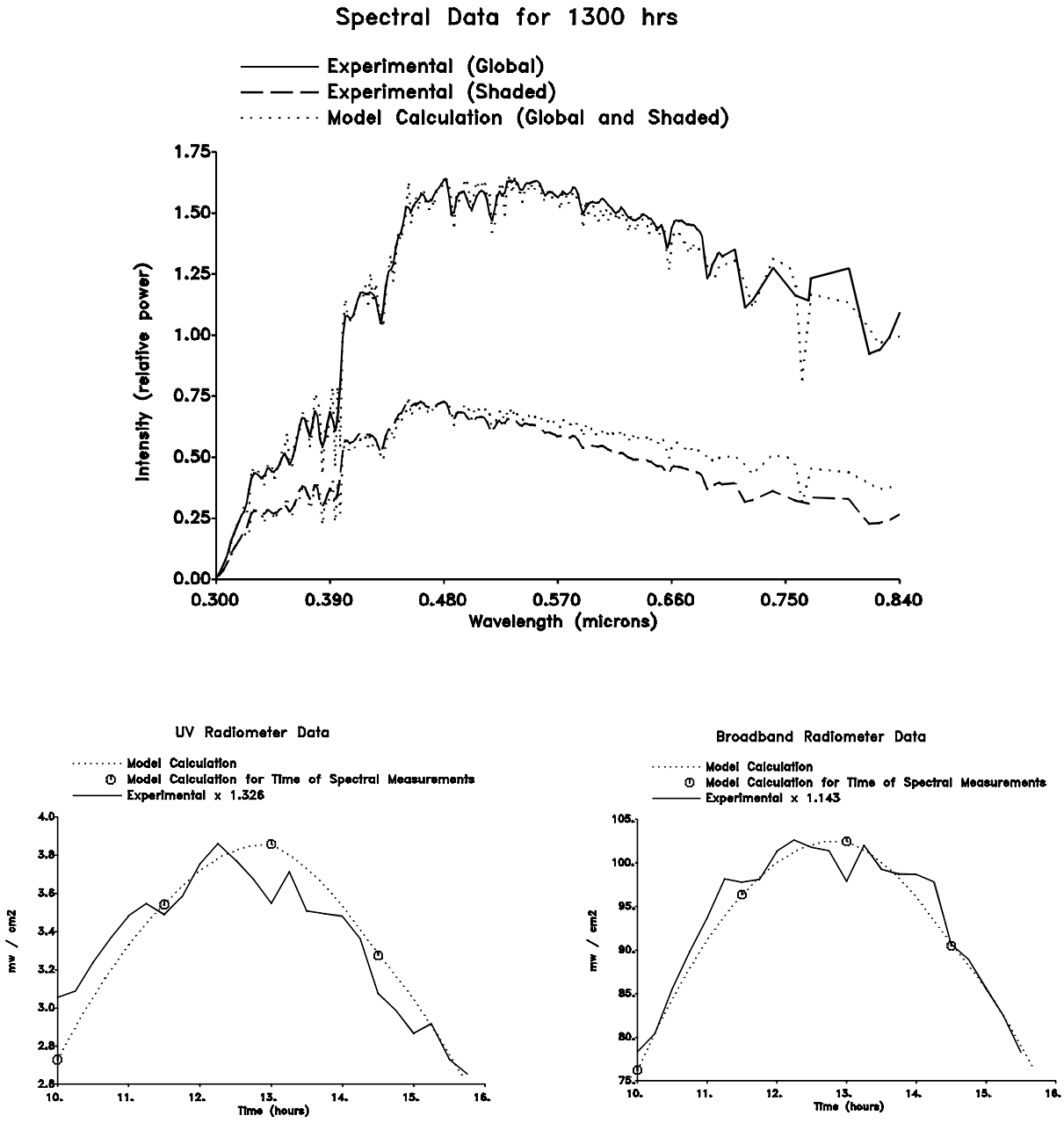

Figure 2. Examples of fits of adjusted solar light model to light characterization data for two outdoor chamber runs. Top plots: fits to direct and diffuse spectral data. Bottom plots: fits to changes with time in the data from the UV and broadband radiometers.

while this method does not directly utilize these data in the photolysis rate calculations, they can be used as a check on the appropriateness of the model's interpolations. Typical results are included on Figure 2, which shows plots of observed and calculated radiometer data vs. time for run OTC-274. In general, the model gave somewhat better predictions of the time profiles of the broadband data than the UV data. This can be attributed to the fact that the spectral response of UV radiometers such as those employed in this study are not particularly well characterized, and the JSPECTRA model uses a highly idealized representation in this regard.

The above procedure predicts light spectra outside the chamber, but the relevant quantities are the light spectra inside the Teflon reaction bag. Jeffries et al. (1989b) measured light reflection and transmission through 2 mil and 5 mil FEP teflon film as a function of wavelength and the incidence angle of the light beam, and developed a parameterized model to fit these data. Although this model includes a term for absorption, the fraction of light absorbed is small (less than 1% for 2-mil film) and can be neglected. Thus only loss due to reflection on the outer chamber walls, or enhancement due to reflection on the inner walls, need be considered. The OTC can be thought of as a transparent bag suspended in space, with light entering it from all directions. If the effect of the presence of the bag on the light coming in from the bottom is neglected, it can be shown that the light enhancement by the reflections from inside the bag just makes up for the light lost due to the reflection when it enters the bag, with the result being that the intensity (and spectrum) inside the bag should be exactly the same as outside. The principle behind this is exactly the same as the principle behind the arguments given by Zafonte et al. (1977) when they concluded that reflections off quartz tubes do not affect results of actinometry measurements using such tubes. Consistent with this is the fact that no significant differences were observed when NO_2 actinometry measurements were made inside and outside the OTC on the same days.

The assumption that the presence of the OTC does not affect light coming from the bottom is not totally valid because the reaction bag is sufficiently close to the ground that all the light coming from the bottom has first passed through the bag, and was thus attenuated by the first reflection from the top. An approximate correction for this was made based on assuming the top and the bottom of the chamber are flat planes of film parallel to the surface, and that the albedo of the carpet under the chamber is the same as the general albedo which is the default in the JSPECTRA model. Parameterized fits to 2-mil FEP Teflon transmission data provided by Jeffries (private communication) were used to calculate the transmissions and reflectance through the chamber walls. This is a fairly small correction, causing the predicted in-chamber photolysis rates to be ~4% than those calculated for outside.

The in-chamber actinic fluxes calculated for every 20 minutes during the run were used as input into model when simulating the run. The model then calculated the photolysis rates for these periods using the absorption cross sections and quantum yields for the various reactions. The photolysis rates

were updated at each time step in the simulation, with the model deriving the photolysis rates for intermediate times between these 20 minute intervals by linear interpolation.

Temperature Characterization

The temperature was observed to varied with time in both the indoor and the outdoor chamber runs, though the variation was much greater in the latter case. The measured temperature data (with any applicable corrections, discussed below), were fit to various straight line segments, and these lines were then used to describe how the temperature varied with time in the model simulations. Subjective judgement was used in determining how many different line segments were required to fit the time variation of the temperature data, but a least squares error optimization program was used to determine the best fit lines once the end points of the line segments have been specified. A single line was sufficient to describe variation in most of the indoor runs, but usually 3-4 lines were required for outdoor runs. For divided chamber runs (OTC and DTC), separate temperature profiles were derived from the data for each side.

The ETC and DTC temperature measurements made with the unshielded probes inside the chamber were used without correction. The XTC temperature measurements made with the aspirated temperature probe were assumed to be accurate and were used without correction. For runs where such data are not available, data taken with the shielded thermocouple inside the chamber were used after being corrected by subtracting 1.5 degrees, as indicated by comparison tests. As discussed above, the in-chamber temperature data for run XTC-083 appear to be anomalous, and the temperature profiles derived for modeling run XTC-086 were also used for modeling this run because the temperature readings in the sampling line were very close for these two runs.

The OTC temperature measurements made with the thermocouple in the sampling line immediately outside the chamber were assumed to be accurate and used without correction. This is applicable to all runs discussed in this report except OTC-270, where unshielded probes inside the chamber were used. There are no data concerning the temperature corrections appropriate for this run. There was also some inconsistency between temperature measurements from the two sides of the chamber. Because of this, this run was modeled with the temperature input varied within its probable uncertainty.

Chamber Radical Source

As discussed elsewhere (Carter et. al, 1982; Carter and Lurmann, 1990, 1991), model simulations of chamber runs must include a representation for a chamber radical source. Although certain runs, especially alkane - NO_x - air runs, are highly sensitive to this parameter, it is less important in affecting results of runs containing complex mixtures designed as atmospheric surrogates, or runs containing species, such as acetone, which are radical initiators. Because of the high sensitivity of alkane - NO_x runs to the chamber radical source (Carter et al., 1979), we carried out n-butane - NO_x - air

irradiations for determining this parameter. The radical source is then adjusted in model simulations to fit the NO oxidation observed in these runs. We found that modeling n-butane runs is a more sensitive method for determining the chamber radical source than analysis of radical tracer - NO_x runs as we have employed previously (Carter et al., 1982).

For the DTC and XTC runs, the chamber radical source parameters were adjusted to fit results of n-butane - NO_x irradiations carried out in those chambers. Based on these results, an OH radical input rate used for both these chambers was 0.06 ppb x the NO_2 photolysis rate. This is lower than the range of values used for the SAPRC ITC (Carter and Lurmann, 1990, 1991), but within the range used for the ETC runs (Carter et al., 1993a).

Since the chamber radical source is expected to be dependent on temperature (Carter et al., 1982), and since temperature varies widely in outdoor runs, use of a temperature-dependent radical source parameter would be appropriate when modeling such runs. Better results in modeling alkane - NO_x runs carried out in the UNC outdoor chamber was obtained when a temperature-dependent radical source was assumed (Carter and Lurmann, 1990, 1991). The three n-butane - NO_x runs carried out in the OTC for this study had average temperatures of 309, 312, AND 317° K, and, if the radical source input parameter (OH input rate / NO_2 photolysis rate — given in units of ppb) is assumed to be independent of temperature, the values which resulted in model simulations best fitting these runs were 0.2, 0.3, and 0.3-0.4 ppb, respectively. All three runs could be fit by assuming the following temperature dependence for the ratio of the OH input flux to the NO_2 photolysis rate: 290°K: 0.02 ppb; 300°K: 0.05 ppb; 310°K: 0.3 ppb; and 320°K: 0.4 ppb. Values for intermediate temperatures were obtained by interpolation. The value for 300° K is based on typical values for indoor runs, and the value for 290° K is an estimate.

Other Chamber-Dependent Parameters

The various other chamber dependent effects which are included in the model simulations of these chamber runs include humidity, dilution, ozone decay rate, initial nitrous acid, NO_x offgasing rates, N_2O_5 hydrolysis, and NO conversion due to background VOCs (Carter and Lurmann, 1990, 1991; Carter et al., 1993a). In the case of the indoor Teflon chambers (the ETC, DTC, and XTC), these were represented in a similar manner as discussed by Carter et al. (1993a) for the ETC, except as follows. The dilution rates were based on decay rates of slowly reacting species in the individual runs, when such data were available. If not, the default dilutions used were those derived from the ETC data (Carter et al., 1993a). No initial nitrous acid was assumed to be present because the NO_x injection procedures employed were designed to eliminate its formation (Carter et al., 1993a).

The chamber-dependent parameters for the OTC runs were the same as used in our previous mechanism evaluation studies using data from this chamber (Carter and Lurmann, 1990, 1991), except that

dilution rates were based on decay rates of slowly reacting observed in individual runs were used when such data were available.

Modeling Incremental Reactivity Measurements

Modeling of incremental reactivity measurements consisted of conducting model simulations of both the base case and the added test VOC experiment, and then analyzing the results using the same procedures as employed experimental data. In the case of the ETC runs, where there is no single base case run associated with any particular test run, the base case simulation associated with a particular test run consisted of modeling the conditions of the that test run, but without the test compound added.

As discussed by Carter et al. (1993a,b), the SAPRC-90 mechanism was found to underpredict the rate of ozone formation in the base case mini-surrogate - NO_x experiments used in conjunction with the ETC acetone reactivity runs. The updates to the mechanism discussed above did not significantly change this. If the model cannot adequately simulate the base case experiments, it cannot be used as a reliable test of mechanisms for test compounds to predict their incremental reactivities in those experiments. Therefore, in the model simulations of the mini-surrogate experiments only, the model for m-xylene in the mini-surrogate was adjusted slightly so the model could better simulate the base case experiment (Carter et al, 1993a,b). The modified m-xylene mechanism is included in the reaction listing in Appendix A. Note that this adjustment was not used in the simulation of the full surrogate runs in the same chamber, since those runs were fit better using the standard m-xylene model (see Results).

EXPERIMENTAL AND MECHANISM EVALUATION RESULTS

The experiments carried out in this program, which were carried out in either the ETC, DTC, XTC, or OTC chamber, consisted of acetone - NO_x, acetone incremental reactivity, acetaldehyde - NO_x, acetaldehyde incremental reactivity, and direct acetone vs ethane comparison runs. In addition, results of selected ethane incremental reactivity experiments are also presented. The conditions and selected results of the single compound experiments are given in Table 1, and the conditions and selected results of the incremental reactivity experiments and their associated base case runs are given in Table 2. Table 2 also gives the conditions and results of the direct acetone vs ethane comparison experiments and the associated side equivalency test run. Plots of selected experimental results, and of results of model simulations of these experiments, are presented in the following sections, where the various types of experiments are discussed in more detail.

Blacklight Chambers

Acetone - NO_x Experiments

Three acetone - NO_x experiments were carried out for this program, one in the ETC and two in the DTC. The runs in the DTC were carried out simultaneously with acetaldehyde - NO_x runs whose results are discussed below. The conditions and results of these experiments are summarized on Table 1, and Figure 3 shows concentration-time profiles of selected species in these experiments. Results of model simulations are also shown. Also shown are results of model simulations with the acetone photolysis quantum yields adjusted as discussed later. It can be seen that the standard model (i.e., the model where the acetone quantum yields are not adjusted) overpredicts the rate of ozone formation in all three of these experiments.

Acetone Reactivity Experiments

A total of seven incremental reactivity experiments with added acetone were carried out in the blacklight chambers, three using the mini-surrogate, two using the full surrogate, and two using the ethene surrogate. Table 2 summarizes the conditions and major results of these experiments, along with the results of the corresponding base case runs. Note that in the case of the ETC experiments only the base case runs carried out immediately before or after the acetone runs are shown on the table, though a much larger number of base case runs were used in establishing the base case conditions (Carter et al., 1993a).

Concentration time profiles for selected species in the base case experiments are shown on Figures 4-6. In all cases the base case experiment were carried out under sufficiently high NO_x (or low ROG/NO_x) conditions that ozone formation is still occurring at the end of the run. This type of

Table 1. Summary of conditions and selected results of the single compound - NO_x - air experiments

VOC	Run	Initial NO_x (ppm)	Initial VOC (ppm)	Average T (°K)	Average k_1 [a] (min^{-1})	Final O_3 (ppm)
Acetone	ETC-445	0.131	7.50	300.9	0.336	0.232
	DTC-54B	0.288	11.15	302.1	0.379	0.205
	DTC-55A	0.147	15.27	301.4	0.379	0.410
	XTC-84	0.237	9.24	302.4	0.233	0.374
	XTC-90	0.194	9.67	305.0	0.233	0.345
	OTC-270B	0.305	5.07	308.5	0.282	0.029
	OTC-273A	0.304	12.11	312.7	0.352	0.928
	OTC-274B	0.272	9.78	307.0	0.349	0.682
Acetaldehyde	DTC-55B	0.146	1.24	301.8	0.379	0.336
	XTC-83	0.251	0.997	302.9	0.233	0.279
	XTC-92	0.257	1.11	302.3	0.233	0.222
	OTC-273B	0.302	1.15	314.3	0.352	0.873
	OTC-274A	0.279	1.08	306.6	0.349	0.725
	OTC-305A	0.272	1.50	315.0	0.309	0.858

[a] NO_2 photolysis rate used in model simulation of run. For indoor runs, value is assigned based on results of NO_2 actinometry experiments. For outdoor (OTC) runs, value shown is average of values calculated as described in the text.

experiment was used for the base case because it represents "maximum reactivity" conditions where VOCs have the greatest effect on ozone formation (Carter, 1991, 1993a,b). It is also particularly useful for mechanism evaluation because it is the most sensitive type of experiment to the effect of the added VOC.

Results of model simulations of the base case experiments are also shown on figures 4-6. It can be seen that the mechanism simulates these experiments fairly well. However, as indicated above, the m-xylene mechanism had to be adjusted to obtain the fits shown for the mini-surrogate runs (Carter et al., 1993a,b). The simulation of the mini-surrogate base case experiment using the unadjusted mechanism is shown on Figure 4 to indicate the effect of this m-xylene adjustment. On the other hand, the available data base of m-xylene - NO_x chamber experiments (Carter and Lurmann, 1990. 1991), and the full surrogate runs carried out in the same chamber (see Figure 4) are better fit by the standard updated SAPRC-90 m-xylene mechanism. This indicates problems with the mechanisms for either m-xylene or the other components of the mini-surrogate, but a discussion of this is beyond the scope of this report.

Table 2. Summary of conditions and results of the incremental reactivity and direct reactivity comparison experiments.

Run	Initial NO_x (ppm)	Initial ROG^{base} (ppmC)	Initial VOC^{test} (ppm)	Avg. T (°K)	Avg. k_1 [a] (min^{-1})	Final $d(O_3-NO)$ (ppm)	Base [b] $d(O_3-NO)$ (ppm)	IR $d(O_3-NO)$ [c]
Mini-Surrogate - NO_x with Added Acetone								
ETC-243	0.463	4.37	0.85	301.8	0.336	0.770	0.748	[d]
ETC-245	0.504	4.65	2.19	302.3	0.336	0.886	0.757	0.059
ETC-247	0.497	4.32	4.15	301.9	0.336	0.942	0.757	0.045
Mini-Surrogate - NO_x with Added Ethane								
ETC-092	0.518	3.73	17.1	301.4	0.343	0.581	0.463	0.007
ETC-099	0.509	3.67	16.6	300.8	0.338	0.562	0.443	0.007
ETC-235	0.494	4.56	43.7	302.0	0.336	1.006	0.754	0.006
Mini-Surrogate - NO_x Base Case [e]								
ETC-091	0.513	3.66	-	301.3	0.344	0.433		
ETC-093	0.520	3.68	-	301.6	0.342	0.473		
ETC-098	0.517	3.58	-	301.4	0.338	0.445		
ETC-100	0.516	3.58	-	301.1	0.337	0.449		
ETC-234	0.504	4.43	-	302.1	0.336	0.727		
ETC-236	0.502	4.39	-	302.0	0.336	0.705		
ETC-242	0.452	4.49	-	301.8	0.336	0.724		
ETC-244	0.484	4.31	-	302.2	0.336	0.707		
ETC-246	0.496	4.44	-	302.2	0.336	0.737		
ETC-250	0.499	4.69	-	299.9	0.336	0.746		
Ethene - NO_x with Added Acetone								
ETC-480	0.419	3.35	3.13	301.4	0.336	1.202	1.146	0.02
ETC-481	0.414	3.05	5.11	301.4	0.336	1.188	1.133	0.01
ETC-490	0.419	3.24	7.97	302.0	0.336	1.259	1.209	0.006
OTC-278A	0.496	1.22	2.85	311.5	0.335	1.170	0.613	0.20
OTC-279B	0.526	2.00	1.27	312.6	0.345	1.317	1.271	0.04
OTC-280A	0.550	2.09	1.99	310.7	0.347	1.397	1.238	0.08
Ethene - NO_x with Added Ethane								
ETC-506	0.407	3.01	50.1	300.6	0.336	1.211	1.033	0.0036

Table 2 (continued)

Run	Initial NO_x (ppm)	Initial ROG^{base} (ppmC)	Initial VOC^{test} (ppm)	Avg. T (°K)	Avg. k_1 [a] (min^{-1})	Final $d(O_3\text{-}NO)$ (ppm)	Base [b] $d(O_3\text{-}NO)$ (ppm)	IR $d(O_3\text{-}NO)$ [c]
Ethene - NO_x Base Case [f]								
ETC-479	0.409	3.36	-	301.4	0.336	1.146		
ETC-482	0.427	3.01	-	301.3	0.336	1.160		
ETC-486	0.440	3.36	-	301.4	0.336	1.082		
ETC-497	0.450	3.68	-	301.9	0.336	1.198		
ETC-505	0.401	3.15	-	301.0	0.336	1.079		
OTC-278B	0.498	1.23	-	312.0	0.335	0.613		
OTC-279A	0.534	1.98	-	312.0	0.345	1.271		
OTC-280B	0.545	2.15	-	311.1	0.347	1.238		
Full Surrogate - NO_x with Added Acetone								
DTC-28A	0.489	4.12	9.37	301.7	0.379	1.056	0.819	0.03
DTC-64B	0.495	4.07	17.08	302.7	0.379	1.120	0.757	0.02
OTC-275A	0.561	4.58	10.48	317.5	0.363	1.565	1.518	0.013
OTC-276B	0.571	4.46	5.81	313.7	0.355	1.498	1.405	[d]
OTC-312A	0.578	4.42	2.16	315.0	0.272	1.285		
OTC-313B	0.494	4.14	1.86	303.4	0.247	0.900		
Full Surrogate - NO_x with Added Ethane								
OTC-312B	0.578	4.65	3.35	315.8	0.272	1.279		
OTC-313A	0.496	4.11	3.26	302.7	0.247	0.853		
Full Surrogate - NO_x Base Case [g]								
DTC-28B	0.492	4.14	-	301.9	0.379	0.819		
DTC-64A	0.494	4.25	-	302.0	0.379	0.757		
OTC-275B	0.625	4.58	-	317.8	0.363	1.518		
OTC-276A	0.580	4.47	-	313.4	0.355	1.409		
OTC-314A	0.577	4.67	-	300.7	0.238	0.749		
OTC-314B	0.576	4.61	-	301.6	0.238	0.755		

[a] NO_2 photolysis rate used in model simulation of run. For indoor runs, value is assigned based on results of NO_2 actinometry experiments. For outdoor (OTC) runs, value shown is average of values calculated as described in the text.

[b] $d(O_3\text{-}NO)$ from base case run. For divided chamber runs with a simultaneous irradiation of a "base case" mixture, this the $d(O_3\text{-}NO)$ from the "base case" side. For single chamber runs, this was derived by estimating the results of a base case run for the conditions of this experiments using linear regressions derived from the results of the base case runs, as discussed by Carter et al. (1993).

Table 2 (concluded)

[c] Incremental reactivity in units of mol O_3 per mol test VOC added
[d] Effect of added VOC too small for meaningful incremental reactivity measure.
[e] Representative runs carried out around the time of the added acetone or ethane experiments. For full listing of runs used in data analysis, see Carter et al. (1993).
[f] The ETC runs are representative runs carried out around the time of the added acetone experiments in that chamber. Results of other runs were very similar. The OTC runs are the base cases for the added acetone carried out at the same time (i.e., with the same OTC run number) but on the other chamber side.
[g] Base cases for the added acetone carried out at the same time (i.e., with the same DTC or OTC run number) but on the other chamber side.

Figures 4-6 also give plots of concentration-time profiles for selected species in the added acetone experiments, along with results of model simulations of these experiments. In addition, Figures 7 and 8 show plots, as a function of irradiation time, of the d(O_3-NO) incremental reactivities which were derived from these experiments. The error bars give the uncertainties in the measured incremental reactivities based on estimated run to run variability and precisions of initial acetone measurements (Carter et al, 1993a). Model simulations of the incremental reactivities are also shown. It can be seen that the model consistently and significantly overpredicts the ozone formation in the added acetone experiments, and thus the incremental reactivity of acetone, regardless of what is being used as the base case ROG surrogate.

Acetaldehyde Experiments

As discussed above, acetaldehyde is a useful VOC for which to compare the results with acetone because, like acetone, it is photoreactive and forms similar products in its reactions. The conditions and selected results of the acetaldehyde - NO_x and the acetaldehyde reactivity experiments are given on Tables 1 and 2, respectively. Note that the acetaldehyde - NO_x run in the DTC was carried out at the same time as an acetone - NO_x run. Much less acetaldehyde is added compared to acetone because of its much greater reactivity.

Figure 9 shows selected results of the acetaldehyde runs carried out in the blacklight chambers. This includes concentration-time plots for selected species in the acetaldehyde - NO_x run and plots of incremental reactivities in the acetaldehyde reactivity experiment. Results of model calculations are also shown. It can be seen that the model gives reasonably good simulations of these data. There may be a slight tendency for the model to overpredict acetaldehyde's reactivity, but the discrepancy is far less than is the case for the acetone experiments.

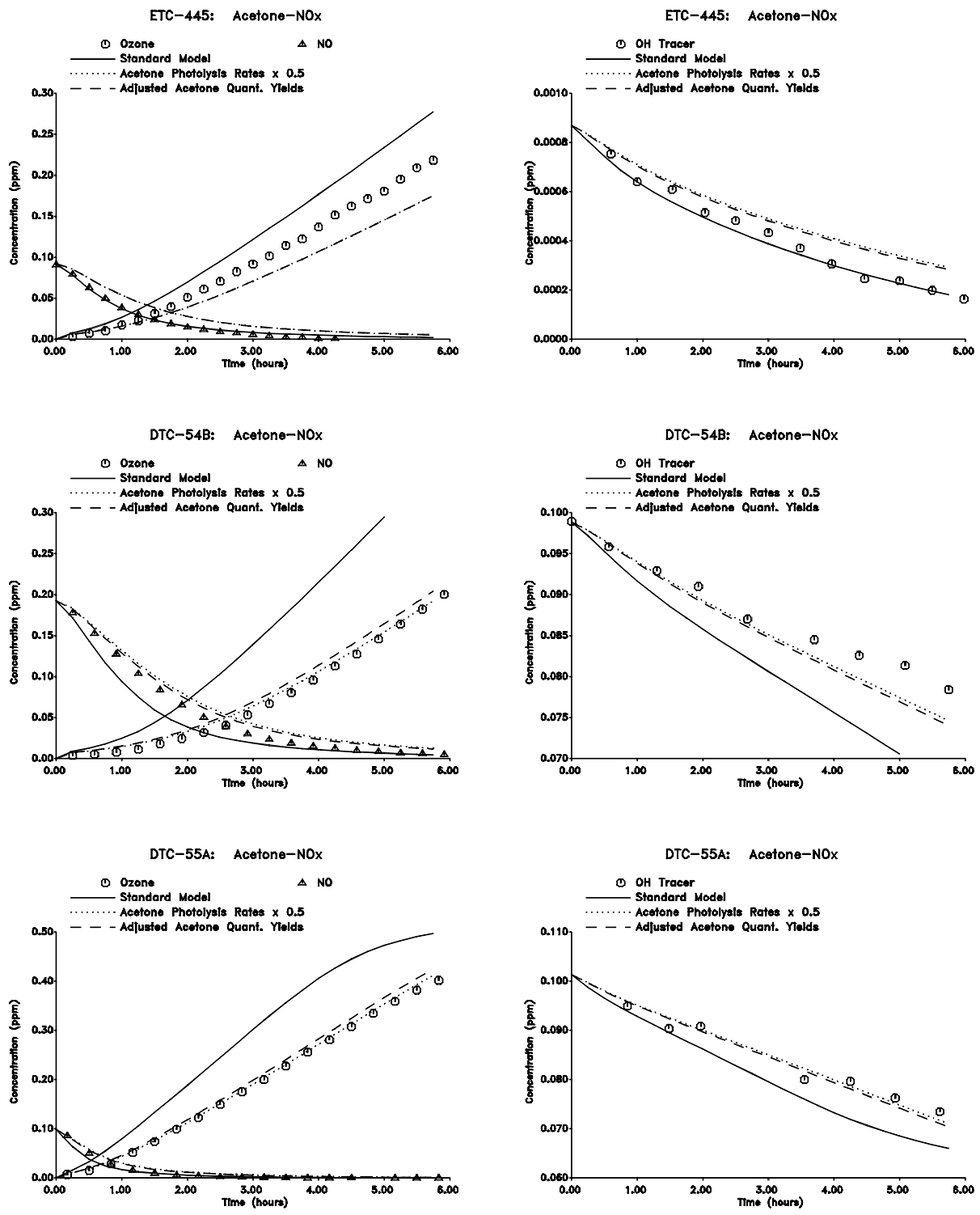

Figure 3. Experimental and calculated concentration-time profiles for selected species in the acetone - NO_x runs carried out in the blacklight chambers.

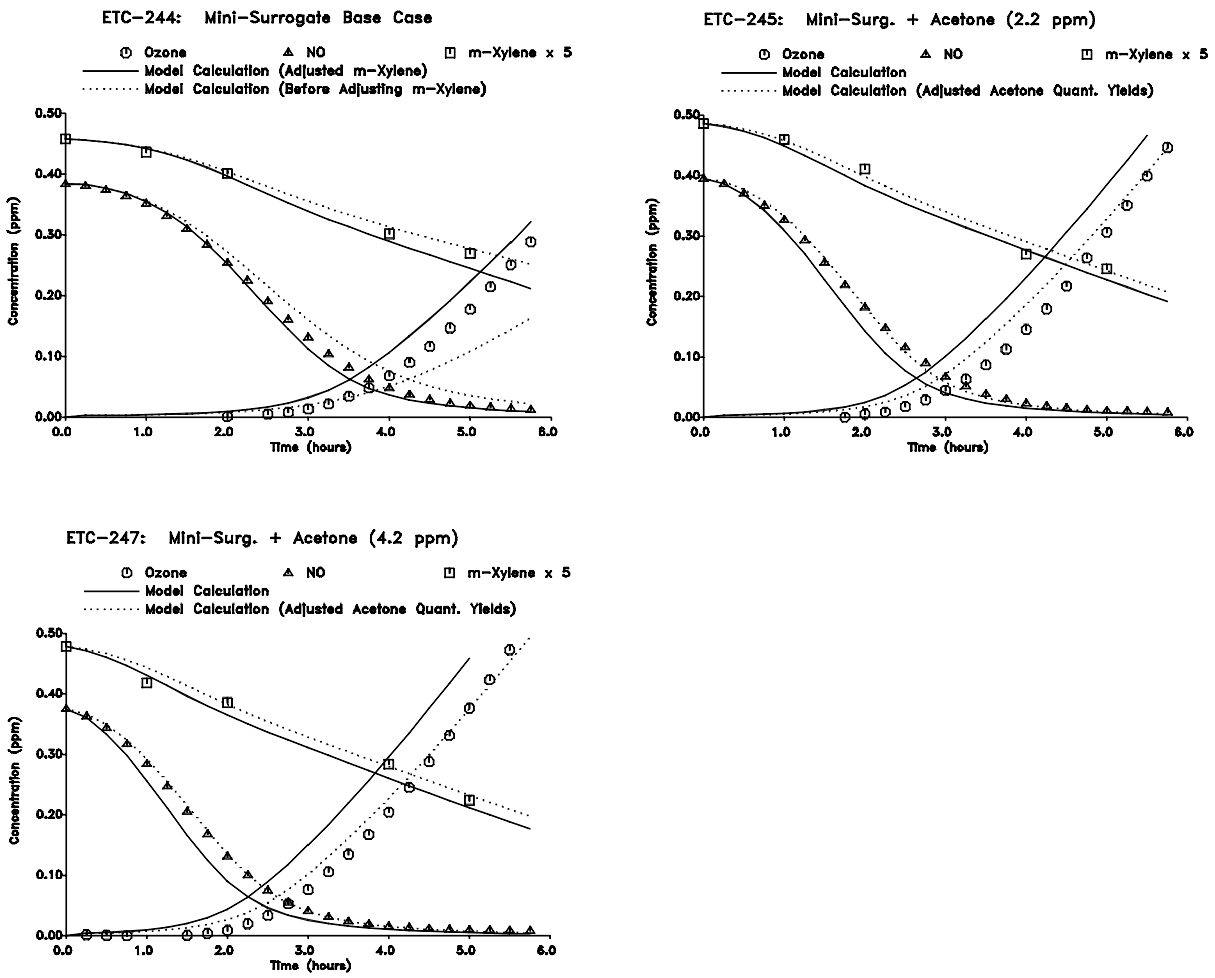

Figure 4. Experimental and calculated concentration-time profiles for selected species in a selected base case run and in the added acetone reactivity experiments using the mini-surrogate in the ETC blacklight chamber.

Ethane Experiments

Since one objective of this study is to assess the reactivities of acetone relative to those of ethane, it is useful to also include available data for ethane. A number of incremental reactivity experiments for ethane were carried out in the ETC using the mini-surrogate, and the results have been presented elsewhere (Carter et al., 1993a). In addition, an ethane reactivity experiment using the ethene surrogate has also been carried out. Table 2 gives a summary of conditions and results of the most reliable ethane reactivity experiments carried out using the mini-surrogate and of the ethane reactivity run using the ethene surrogate, and Figure 10 gives plots of the experimental and calculated incremental reactivities for of these runs. (Runs carried out before the NO_x injection system was modified to remove

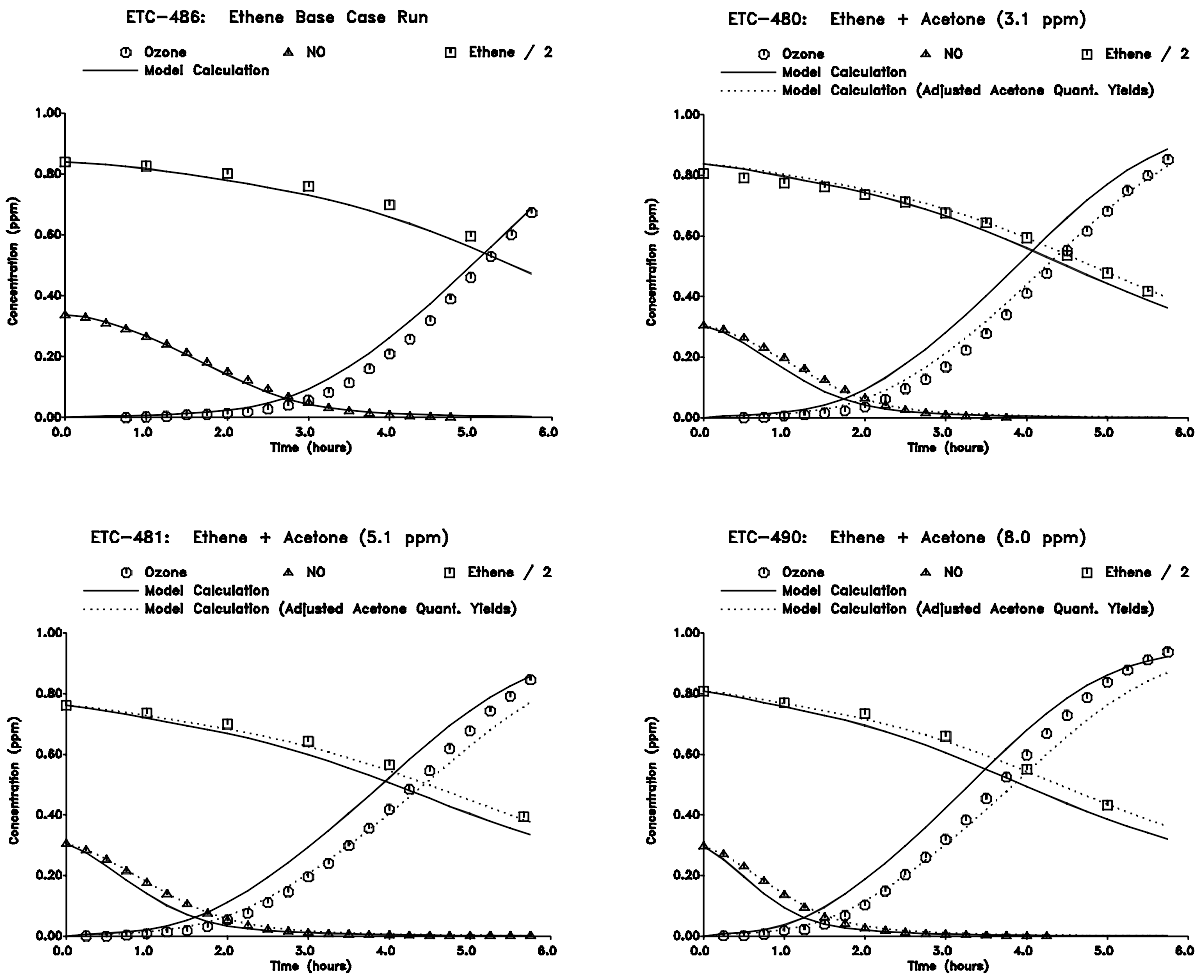

Figure 5. Experimental and calculated concentration-time profiles for selected species in a selected base case run and in the added acetone reactivity experiments using the ethene surrogate in the ETC blacklight chamber.

nitrous acid contamination, and runs which had anomalously high reactivities which can be attributed to an impure ethane sample, are not shown. See Carter et al., 1993.)

It can be seen that the model simulates the ethane reactivity measurements quite well. This is expected given that ethane's reaction mechanism is not considered uncertain, and the fact that ethane's major oxidation product is acetaldehyde, whose reactions the model apparently simulates quite well.

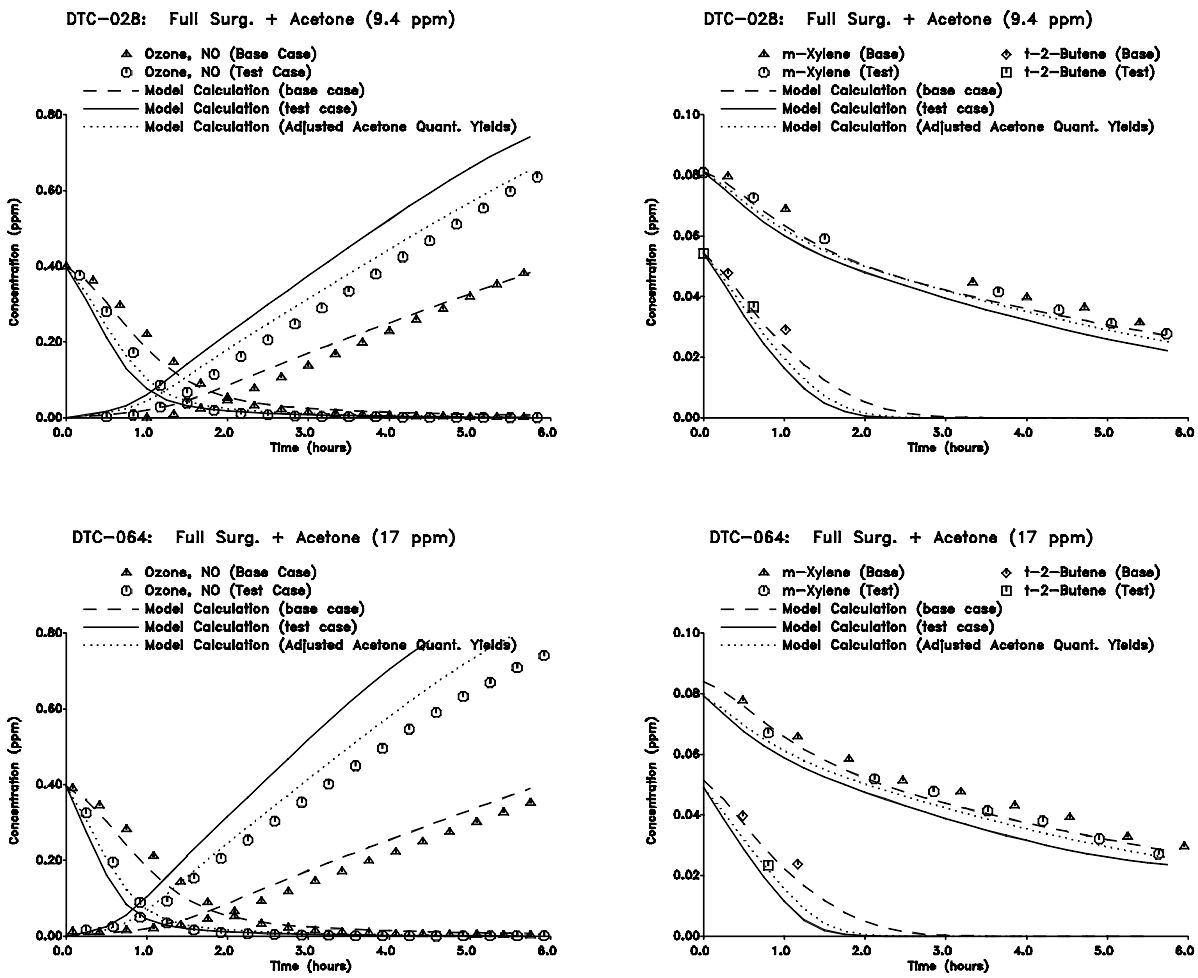

Figure 6. Experimental and calculated concentration-time profiles for selected species in a in the added acetone reactivity experiments using the full surrogate in the DTC blacklight chamber.

Xenon Chamber

Acetone - NO_x Experiments

Two acetone - NO_x experiments were carried out using the XTC chamber with the xenon arc light source. The conditions and selected results of the acetone - NO_x experiments are summarized on Table 2, and concentration-time plots of selected species are shown on Figure 11. Results of model calculations are also shown. It can be seen that, in contrast with the results with the blacklight chambers, the standard model may be biased towards underestimating the reactivity of acetone. The model fits the data well in one run, but underpredicts ozone somewhat in the other. The model with the photolysis rates

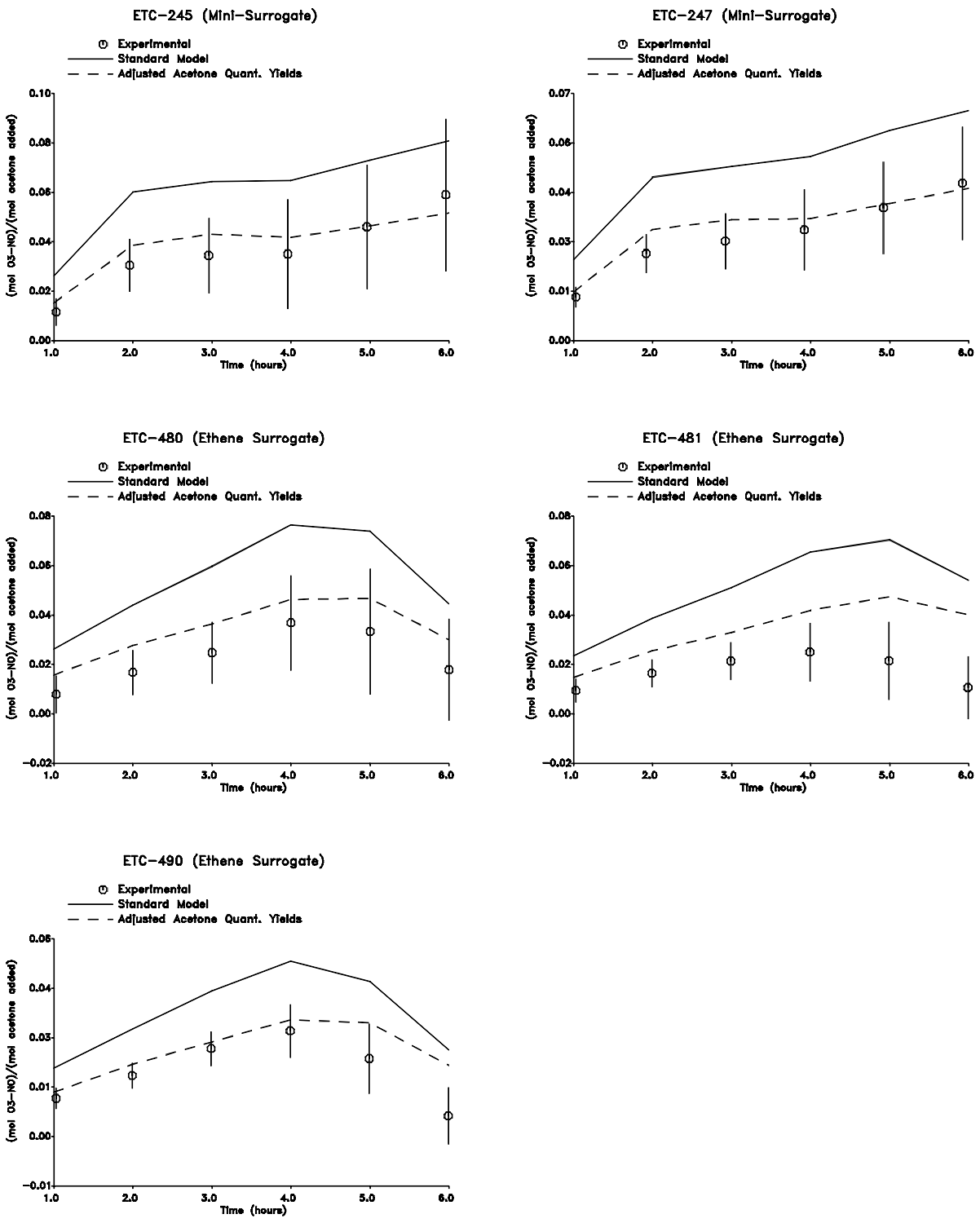

Figure 7. Experimental and calculated incremental reactivities, as a function of reaction time, in the added acetone reactivity experiments using the mini-surrogate and the ethene surrogate in the ETC blacklight chamber.

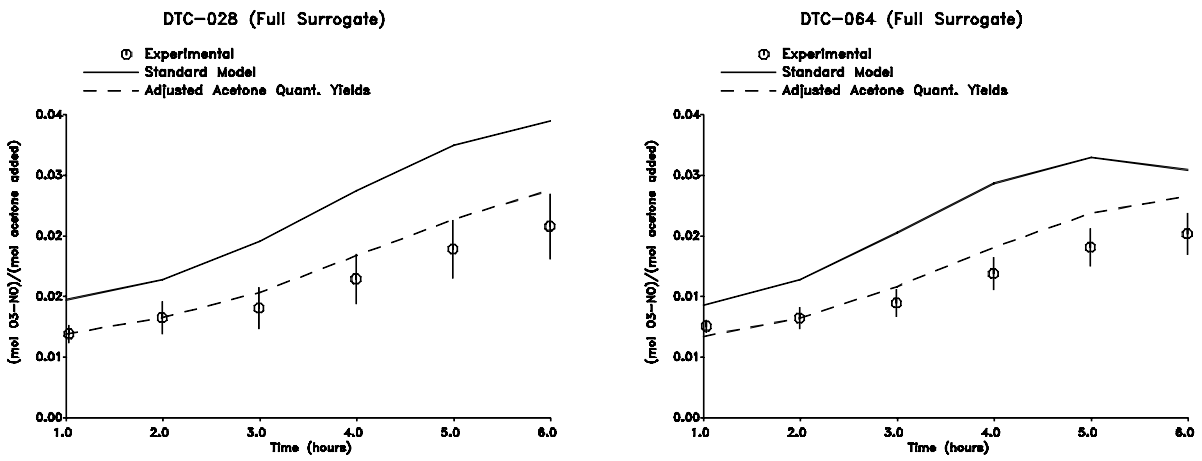

Figure 8. Experimental and calculated incremental reactivities, as a function of reaction time, in the added acetone reactivity experiments using the full surrogate in the DTC blacklight chamber.

reduced by a factor of two significantly underpredicts the ozone formation and radical levels in both these experiments.

Acetaldehyde - NO_x Experiments.

For comparison and control purposes, we also carried out acetaldehyde - NO_x experiments in this chamber. The conditions and selected results of the acetaldehyde - NO_x experiments are summarized on Table 2, and concentration-time plots of selected species are shown on Figure 12. Results of model calculations are also shown. It can be seen that, as with the blacklight chamber runs, the model fits the data very well.

Outdoor Chamber

Acetone - NO_x Experiments

A total of six acetone - NO_x experiments were conducted in the outdoor chamber for this program, of which three are used for mechanism evaluation. The conditions and selected results of these runs are summarized on Table 2. Three of these runs were carried out on overcast days, and since our procedures for light characterization for outdoor runs is not applicable for such conditions they were not modeled. Concentration-time plots for selected species for the other three runs are shown on Figure 13, where they can be compared with the model predictions. Note that run OTC-270 was carried out in November of 1992, while the other two runs were carried out in June of 1993.

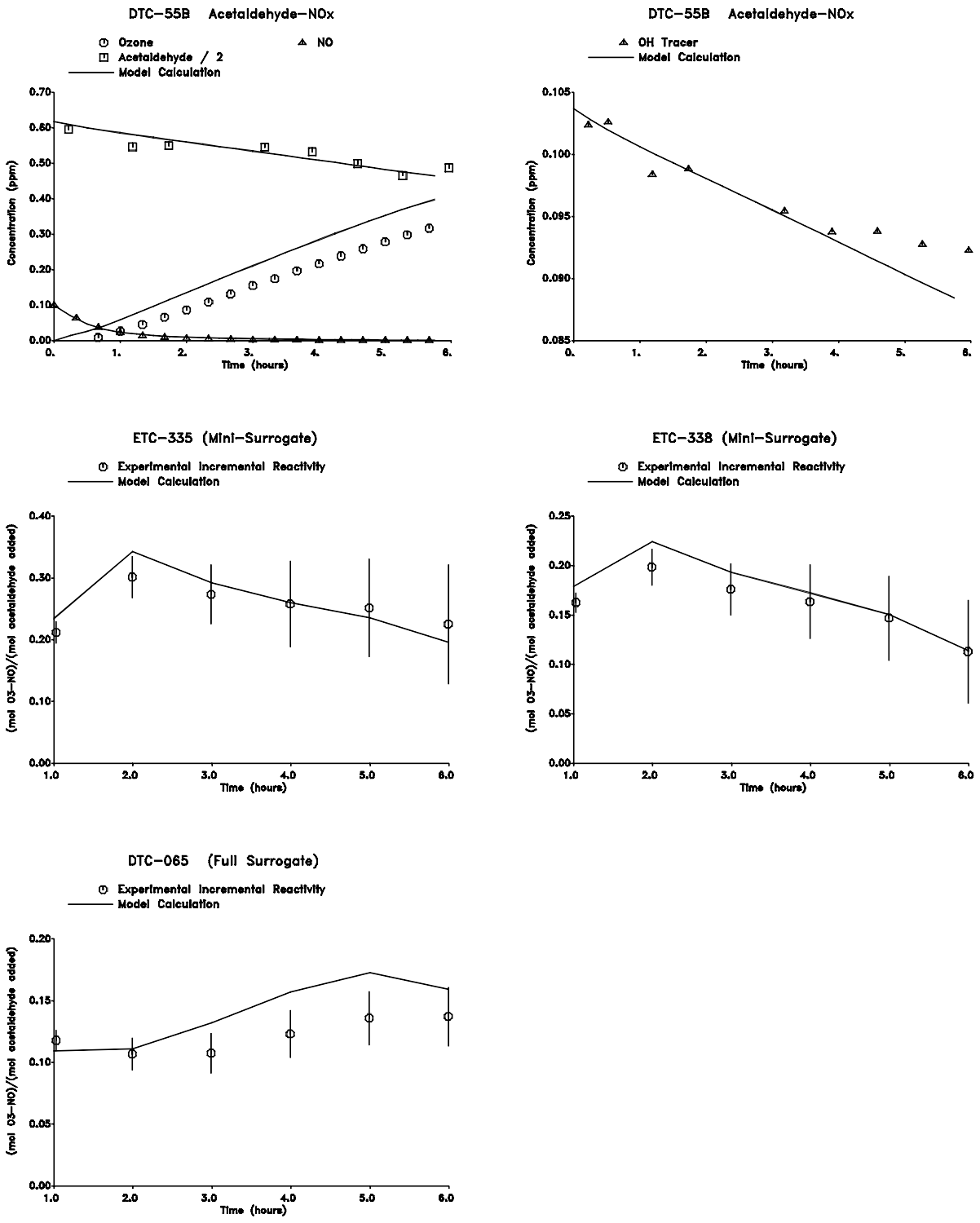

Figure 9. Selected experimental and calculated results for the acetaldehyde - NO_x experiments and the added acetaldehyde reactivity experiments carried out using the blacklight chambers.

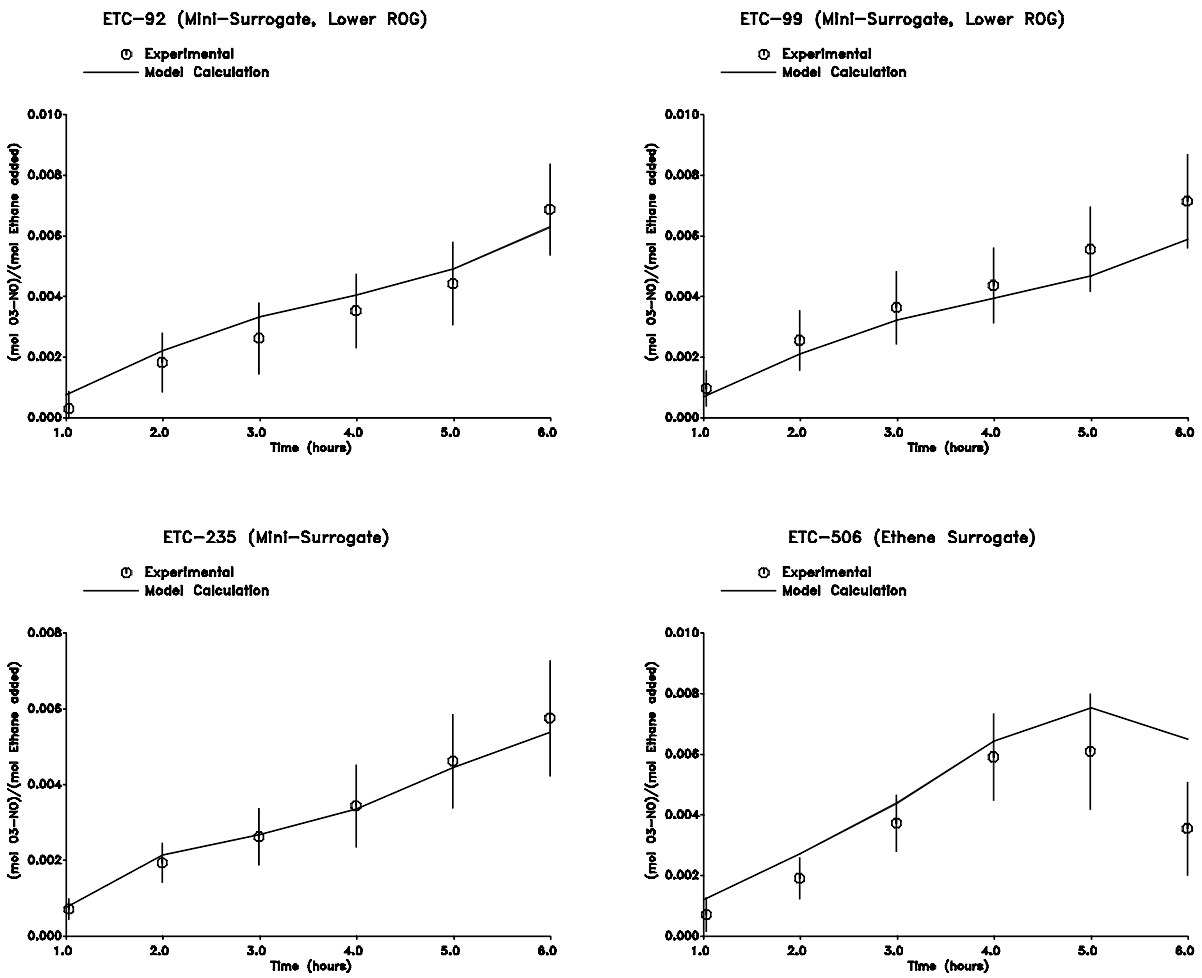

Figure 10. Experimental and calculated incremental reactivities, as a function of reaction time, in the added ethane reactivity experiments. All experiments were carried out in the ETC blacklight chamber.

It can be seen that the model simulation overpredicts the ozone formation and NO oxidation rates in the winter run (OTC-270), but fits data in the summer runs reasonably well. Although the temperatureis somewhat uncertain in run OTC-270, adjusting the temperature within its estimated uncertainty does not significantly improve the model simulation.

Acetaldehyde - NO_x Experiments.

As with the XTC, acetaldehyde - NO_x experiments were carried out in the outdoor chamber for control and comparison purposes. The conditions and selected results of the acetone - NO_x experiments are summarized on Table 2, and concentration-time plots of selected species are shown on Figure 14. Results of model calculations are also shown. It can be seen that, as with the runs in the

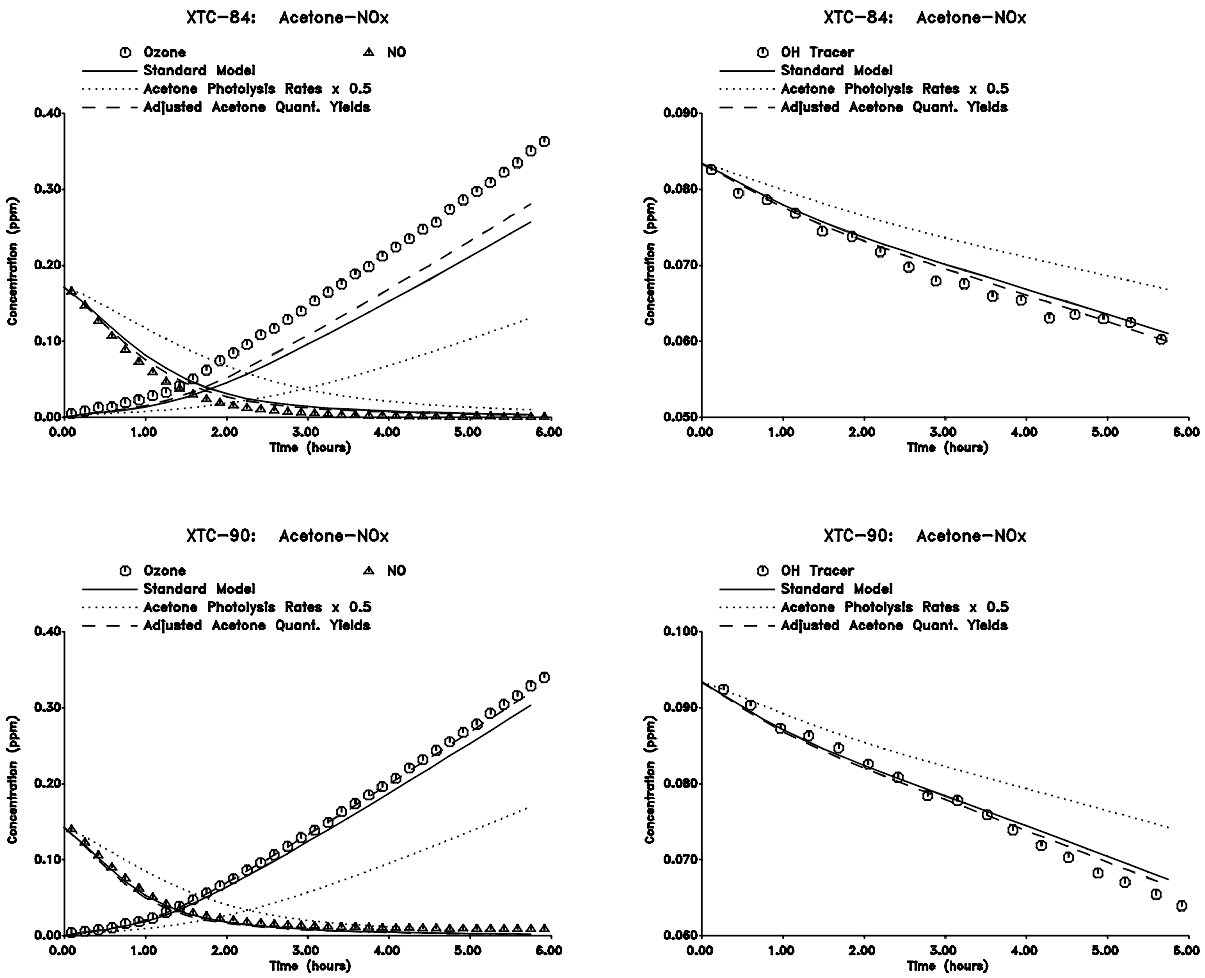

Figure 11. Experimental and calculated concentration-time profiles for selected species in the acetone - NO_x runs carried out in the xenon arc chamber.

other chamber, the model fits the data very well. This is particularly gratifying in this case, given the greater uncertainties and difficulties in characterizing light conditions for outdoor runs. However, all the acetaldehyde runs were carried out in the summer, and thus these data give no indication of the ability of the model to simulate conditions in winter runs.

Acetone Reactivity Experiments

Two acetone reactivity experiments were carried out using the full surrogate and three using the ethene surrogate. The conditions and selected results of these runs are summarized in Table 1, concentration-time plots for selected species are given on Figure 15 for runs using the full surrogate